

Copy No. 10

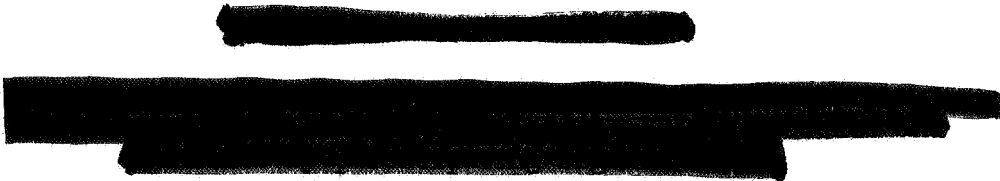
NASA Project Apollo Working Paper No. 1090

AN INVESTIGATION OF STATIC FLOTATION
CHARACTERISTICS OF APOLLO COMMAND MODULE



FACILITY FORM 602

N70-75878
 (ACCESSION NUMBER) (THRU) Non
 (CODE)
 (CATEGORY)
 39
 (PAGES)
 TMX-65143
 (NASA CR OR TMX OR AD NUMBER)

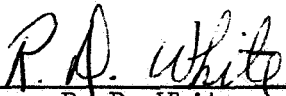


NATIONAL AERONAUTICS AND SPACE ADMINISTRATION
MANNED SPACECRAFT CENTER
Houston, Texas
September 9, 1963

NASA PROJECT APOLLO WORKING PAPER NO. 1090

AN INVESTIGATION OF
STATIC FLOTATION CHARACTERISTICS OF
APOLLO COMMAND MODULE

Prepared by:


R. D. White
Aerospace Technologist

Authorized for Distribution


Maxime A. Faget
Assistant Director
For Engineering and Development

NATIONAL AERONAUTICS AND SPACE ADMINISTRATION
MANNED SPACECRAFT CENTER
HOUSTON, TEXAS
SEPTEMBER 9, 1963

LIST OF FIGURES

Figure	Page
1 Details of Apollo Command Module Configuration at Touchdown	6
2 Details of Pressure Vessel	7
3 Apollo External Configuration Model Test Set-up	8
4 Apollo Pressure Vessel Model Test Set-up	9
5 Typical Force Diagram on Pressure Vessel Model Drawing .	10
6 Buoyancy Force Lines of Action - Vertical Centerline Intersection vs Angle of Heel for Test Models at 8,500 Pounds Displacement	11
7 Buoyancy Force Lines of Action - Vertical Centerline Intersection vs Angle of Heel for Test Models at 9,000 Pounds Displacement	12
8 Buoyancy Force Lines of Action - Vertical Centerline Intersection vs Angle of Heel for Test Models at 9,500 Pounds Displacement	13
9 Buoyancy Force Lines of Action for Pressure Vessel at 8,500 Pounds Displacement	14
10 Buoyancy Force Lines of Action for Pressure Vessel at 9,000 Pounds Displacement	15
11 Buoyancy Force Lines of Action for Pressure Vessel 9,500 Pounds Displacement	16
12 Buoyancy Force Lines of Action for External Configuration at 8,500 Pounds Displacement	17
13 Buoyancy Force Lines of Action for External Configuration at 9,000 Pounds Displacement	18
14 Buoyancy Force Lines of Action for External Configuration at 9,500 Pounds Displacement	19

Section	Page
15 Righting Moment vs Angle of Heel for Pressure Vessel and External Configuration at 8500 Pounds Displacement with C.G. Located at $X_c = 45$, Offset 7.5 inches	20
16 Righting Moment vs Angle of Heel for Pressure Vessel and External Configuration at 9,000 Pounds Displacement with C.G. Located at $X_c = 45$, Offset 7.5 inches	21
17 Righting Moment vs Angle of Heel for Pressure Vessel and External Configuration at 9,500 Pounds Displacement with C.G. Located at $X_c = 45$, Offset 7.5 inches	22
18 Regions of Significant C.G. Locations for Pressure Vessel and External Configuration at 8,500 Pounds Displacement	23
19 Regions of Significant C.G. Locations for Pressure Vessel and External Configuration at 9,000 Pounds Displacement	24
20 Regions of Significant C.G. Locations for Pressure Vessel and External Configuration at 9,500 Pounds Displacement	25
21 C.G. Regions of Determinate and Non-Determinate Attitudes at 8,500 Pounds Displacement	26
22 C.G. Regions of Determinate and Non-Determinate Attitudes at 9,000 Pounds Displacement	27
23 C.G. Regions of Determinate and Non-Determinate Attitudes at 9,500 Pounds Displacement	28
24 Waterline and Spacecraft Centerline Intersection at 8,500 Pounds Displacement	29
25 Waterline and Spacecraft Centerline Intersection at 9,000 Pounds Displacement	30
26 Waterline and Spacecraft Centerline Intersection at 9,500 Pounds Displacement	31

Section	Page
27 Typical Apollo Flotation Attitudes and Hatch Exposure at 9,000 Pounds Displacement with C.G. Located at $X_c = 45$, Offset 7.5 inches	32
28 Typical Apollo Flotation Attitudes and Hatch Exposure at 9,000 Pounds Displacement with C.G. Located at $X_c = 42$, Offset 10 inches	33

SUMMARY

An investigation of the static flotation characteristics of the present Apollo configuration was conducted using one-fifth geometrically scaled models of the command module and its pressure vessel. The resulting data were expanded graphically and analytically to arrive at the flotation characteristics. Results from this study show that the presently considered Apollo concept will have desirable static flotation characteristics with proper location of the center of gravity.

INTRODUCTION

Because of the possibility of a water landing after reentry of an Apollo Command Module, it is necessary to be able to predict the flotation characteristics of the module; lack of such an investigation in the Mercury program caused some problems late in the design stage. Design of a spacecraft must be such as to allow the hatch to be above water at all stable angles of heel (list angles). Previous investigations at the Manned Spacecraft Center on post-landing hydrostatic flotation characteristics of an earlier Apollo module concept have been conducted, but since then the Apollo configuration has changed considerably. The work described herein deals with the present concept.

The objectives of this study were to obtain and evaluate the static flotation characteristics of the current Apollo command module configuration for any predicted spacecraft center of gravity (c.g.) location. Flotation characteristics are defined as the stable attitude or attitudes attainable at post-landing conditions for any c.g. location and the resulting waterline locations.

DESCRIPTION OF APPARATUS

Two fiberglass models were used to obtain the basic data required for the flotation characteristics. One was a one-fifth geometrically scaled model of the external Apollo command module configuration. The second was a one-fifth scale model of the pressure vessel exterior. Full scale dimensions of each configuration are presented in figures 1 and 2, respectively. The necessity of using two models was due to the consideration that the exterior Apollo shell at touchdown will not be watertight. This means that the buoyancy effect will be due to the shape of the pressure vessel plus the buoyancy of the submerged outside structure and all submerged equipment, tanks, et cetera, that will occupy the space

between the two structures.

Each model was encircled by a steel ring contained in a vertical plane through the axis of symmetry. The rings had holes at prescribed intervals to allow attachment of an external weight at any desired location. The model-ring combinations with externally attached weights are shown in figures 3 and 4.

At present it is estimated that the weight of the actual command module will be between 8,500 and 9,500 pounds at touchdown. The simulated weights at which each model was floated were in this range. In any model analysis the weight scale factor is the cube of the model scale. Therefore, in the case of the one-fifth model scale, the weight scale factor is $\frac{1}{125}$. Since the tests were run in fresh water, all model weights were adjusted to sea water conditions by dividing each test setup weight by the specific gravity of sea water (1.026). Hence, the required scaled weights were from 66 to 74 pounds. Both models were designed to weigh less than the required test weights, thus allowing the addition of external weights to bring the models up to the desired simulated weight.

PROCEDURE

Before starting the tests the weight and c.g. location for each model-ring were obtained. The external weight was attached to the ring; then the model was placed in a tank of water and allowed to attain a stable attitude. During each test the external weight was submerged at all times so that the buoyancy force on the weight had to be taken into consideration. The buoyancy effect of that portion of the steel ring which was submerged was neglected since it was less than 0.5 percent of the model displacement. After the required data were recorded, the weight was then attached to the next prescribed hole in the ring. This forced the model to take a new angle of heel at the same weight. Thus, in effect, the c.g. of the simulated spacecraft had been moved. Data were obtained through 180 degrees of heel for each model. For each position the location of the suspended weight and the points of intersection of the waterline on the ring were recorded. This procedure was followed for simulated weights of 8,500, 9,000, and 9,500 pounds. The position of the waterline, the model c.g. location, and the point of attachment of the external weight at each attitude were located on full-scale drawings of the models and rings. Since all weight force vectors acted perpendicular to the waterline, an analytical summation of moments and of forces revealed the line of action of the buoyancy force on the model. Because the system was stable, this buoyancy force line of action acted through the composite c.g. of the complete system. (Figure 5 is a representation of one of these drawings.) Therefore, with the actual spacecraft c.g. located at

any point on the line of action, the spacecraft would attain the angle of heel of that particular attitude.

RESULTS AND DISCUSSION

From the drawings, the location of the intersection of the buoyancy force line of action with the spacecraft geometric centerline was determined for each attained angle of heel. This is point A on figure 5. With this information a plot was made of the angle of heel between 0 and 180 degrees versus the recorded intersection points (or stations) for each model and test displacement. The results are shown in figures 6 through 8.

Graphs (figures 9 through 14) were made with the ordinates representing the stations on the centerline of the spacecraft (X_c), and the buoyancy force lines of action at 5 degree and 10 degree intervals were drawn from each corresponding intersection of the centerline as obtained from the previous curves. The abscissas represent perpendicular distances from the spacecraft centerline. Thus, in effect, the drawings are half sections of the pressure vessel and external configuration with the correct buoyancy lines of action drawn in at prescribed angles for the three different weights.

A spacecraft c.g. can be placed at any location on these drawings. With any c.g. located, the righting or upsetting lever arm can be measured; this arm would be the perpendicular distance from the c.g. to the desired buoyancy force line of action. To obtain the righting or upsetting moment at any angle, the perpendicular distance is multiplied by the spacecraft weight. By placing the c.g. at a desired location, a plot of righting moment versus angle of heel can be drawn by obtaining the data as illustrated above. Examples for such a plot are figures 15 through 17. The c.g. location used in these examples is in the vicinity currently being considered for the actual Apollo command module. When making the plot, clockwise moments were assumed negative. Also, assuming that the Apollo c.g. will always seek the lowest plane attainable with reference to the water surface, the angle of heel was plotted to only 180 degrees because any angle of heel greater than 180 degrees will cause the spacecraft to turn on its axis of symmetry and thus duplicate flotation characteristics. If an evaluation of a specific c.g. location is desired, full size reproductions of figures 9 through 14 are available upon request from Systems Evaluation and Development Division of the Manned Spacecraft Center.

From the righting moment versus angle of heel curves, the stable attitudes of the floating module can be found. Any stable position

exists where the force of gravity is in direct line with the force of buoyancy. The stable attitudes exist on the curves where the righting moment curve crosses the zero moment line with a positive slope. The module is theoretically stable where the curve crosses the zero moment line with a negative slope, but any minute change in attitude would cause the spacecraft to seek one of the true stable positions. Positive righting moments will decrease the angle of heel, and negative righting moments will increase the angle of heel. With the outside configuration curve and the pressure vessel curve superimposed on the same graph, it can be seen that the actual righting moment curve would lie somewhere between the two.

When analyzing significant c.g. location regions, reference should be made to figures 9 through 14. By fairing the intersections of the buoyancy force lines of action, c.g. boundary extremes are obtained for estimating the number of stable attitudes. This shows that there are three regions of c.g. location which result in significantly different flotation attitudes and a region of indeterminable attitude or attitudes. The regions shown in figures 18 through 20 are the three determinable regions (1 through 3) of the outside configuration compared with those of the pressure vessel. Figure 21 through 23 show the outside configuration and pressure vessel regions superimposed, and thus illustrate the existence of a non-determinate region 4. As stated previously, with the undefined buoyancy effects of all equipment, tanks, et cetera, around the outside of the pressure vessel, the floating attitudes of a c.g. location in region 4 cannot be fully defined. With the c.g. located anywhere in region 4, the spacecraft will have either one or two stable attitudes and an angle of heel which cannot be estimated and can be anywhere between 0 and 180 degrees. With the c.g. located at any point in region 1, the module will have one stable attitude with a predictable angle of heel somewhere between 0 and 90 degrees. With the c.g. located anywhere in region 2, there will be only one stable attitude with the angle of heel between 90 and 180 degrees. The pressure vessel curve of figure 17 is an example of the righting moment curve for a c.g. located in region 2 (angle of heel is 144°). If the c.g. is located at any point in region 3, the spacecraft will have two stable attitudes; one attitude will have an angle of heel between 0 and 90 degrees, and the second will be between 90 and 180 degrees. Figures 15 and 16 are examples of the righting moment curves for a c.g. location in region 3.

With the information given in figures 24 through 26, one can pictorially determine what portion of the spacecraft is below the surface of the water for each weight at different angles of heel. At angles where the model centerline and the waterline were in planes almost parallel to each other the centerline-waterline intersection was not obtainable (heel angles of 80° through 110°). Figures 27 and 28 show the typical flotation attitudes for the Apollo with the c.g. located in region 3 at $X_c = 45$ offset

7.5 inches and at $X_c = 42$ offset 10 inches, respectively.

CONCLUDING REMARKS

From the study, it can be stated that there are three significant regions which give different flotation attitudes and one non-determinate region. With the presently considered Apollo command module c.g. location and weight, there are two stable attitudes. Results from this study show that the presently considered Apollo concept will have desirable static flotation characteristics with proper c.g. location. Once a weight and c.g. location are established, the waterline and angle of heel can be closely predicted with the information from this study.

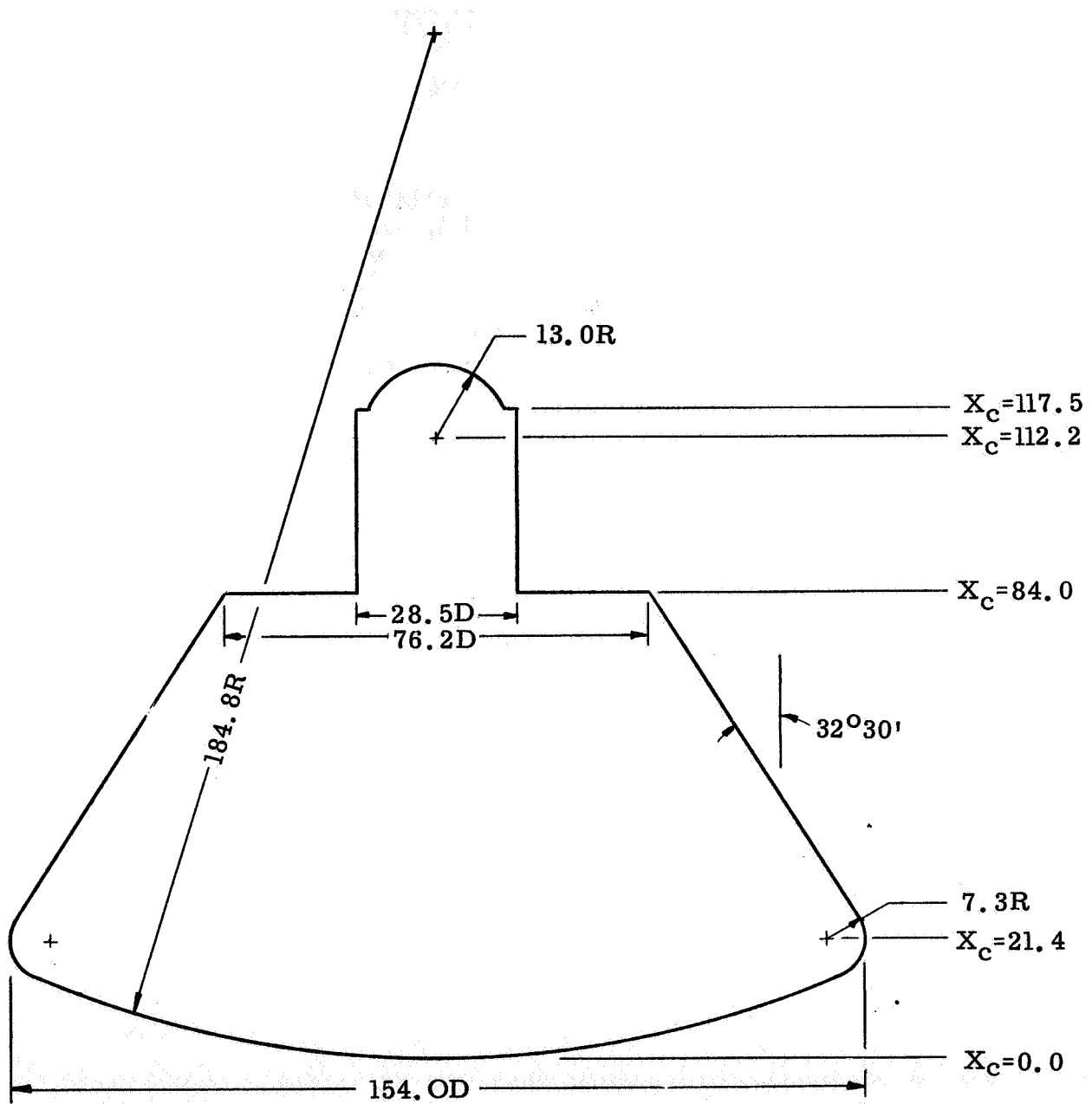


FIG. 1 DETAILS OF APOLLO COMMAND MODULE CONFIGURATION AT TOUCHDOWN

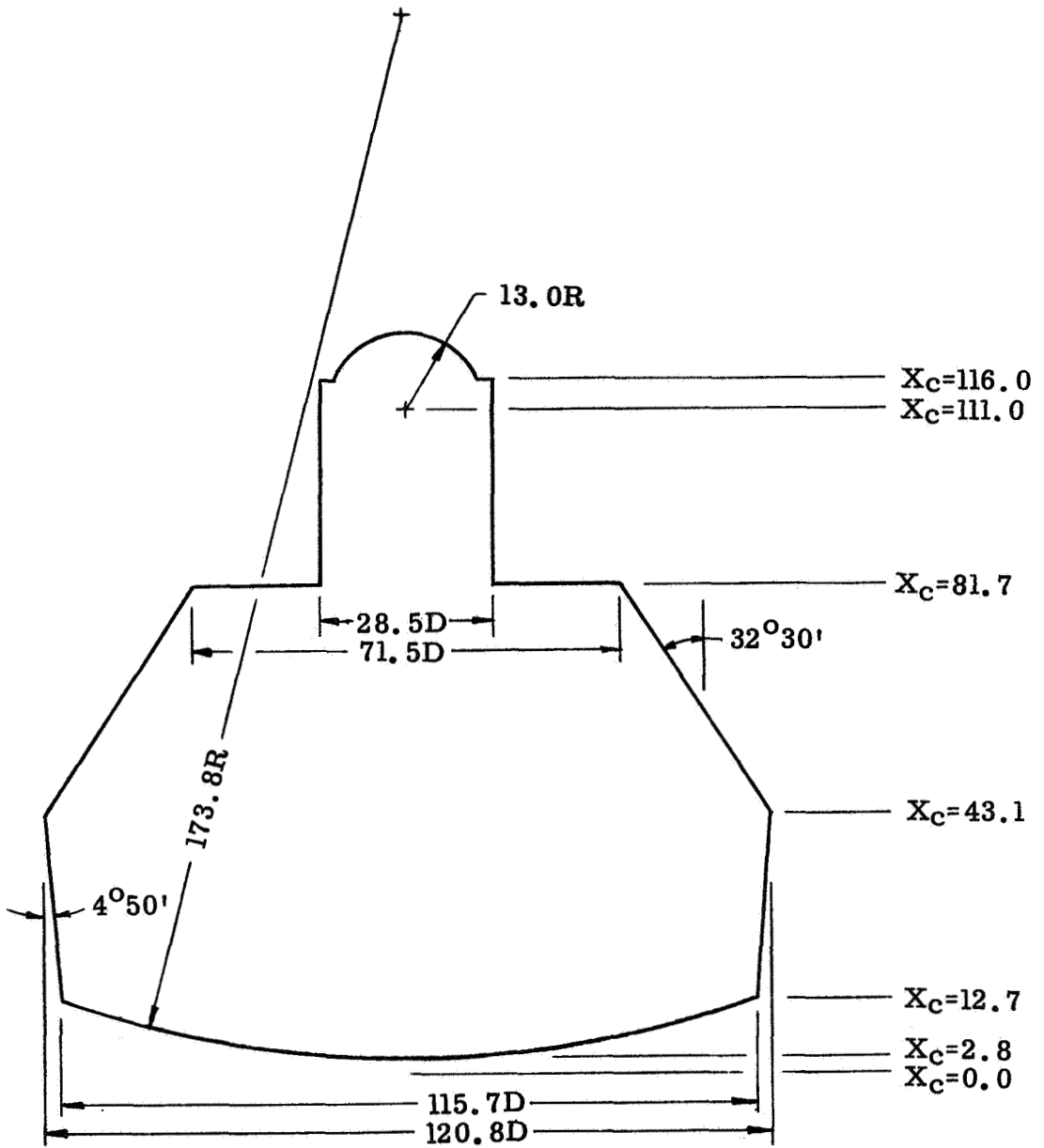


FIG. 2 DETAILS OF PRESSURE VESSEL

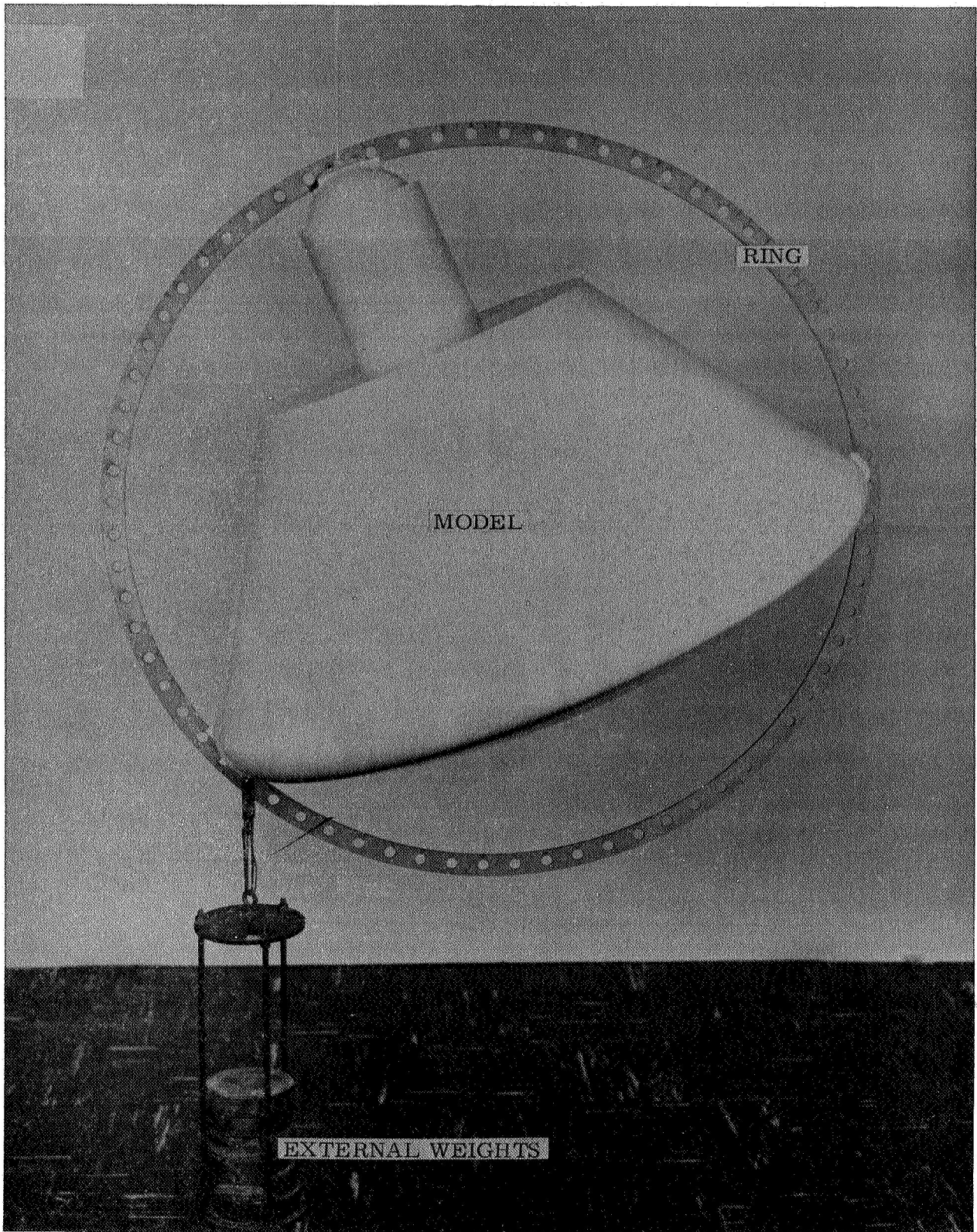


FIG. 3 APOLLO EXTERNAL CONFIGURATION
MODEL TEST SET-UP

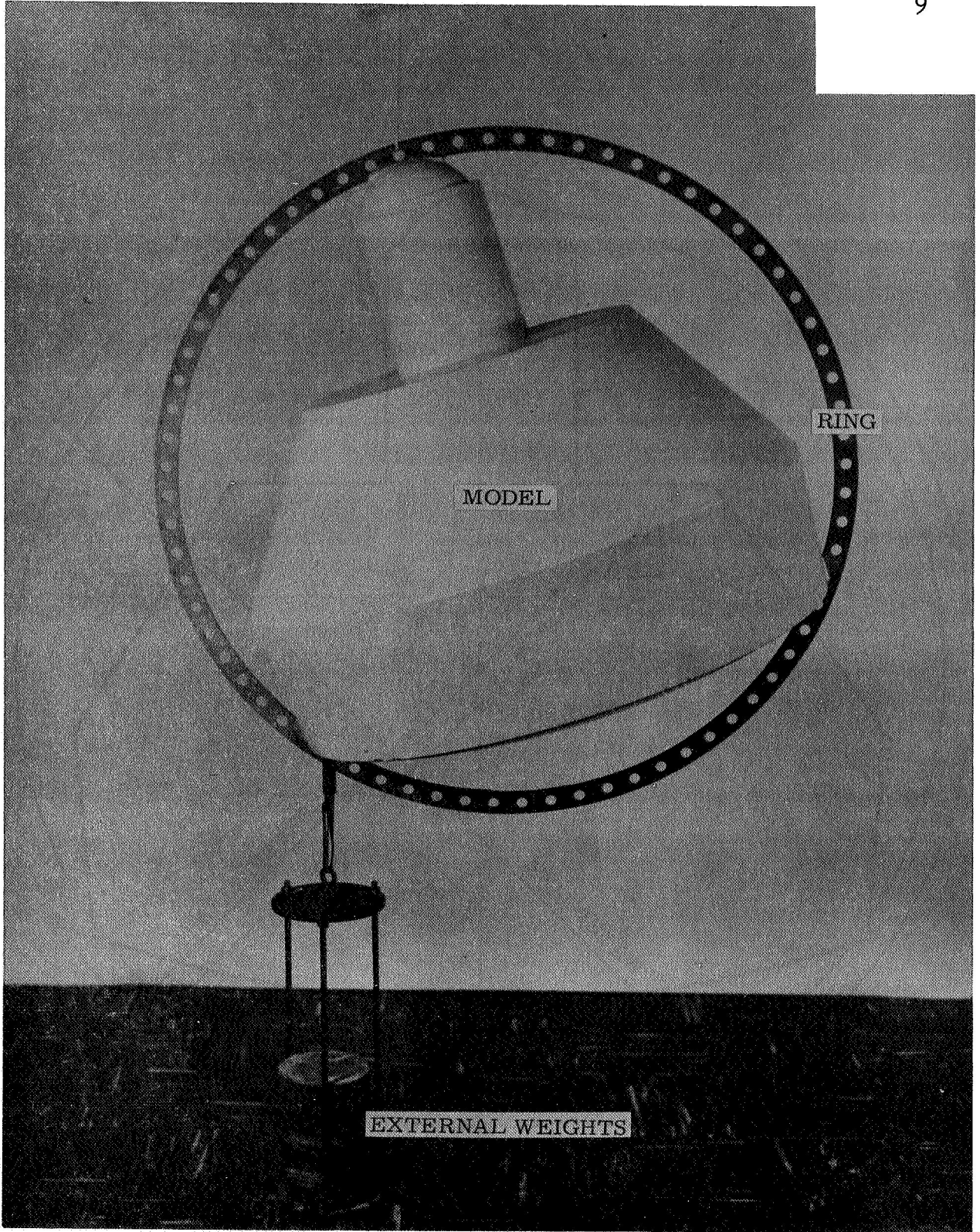


FIG. 4 APOLLO PRESSURE VESSEL
MODEL TEST SET-UP

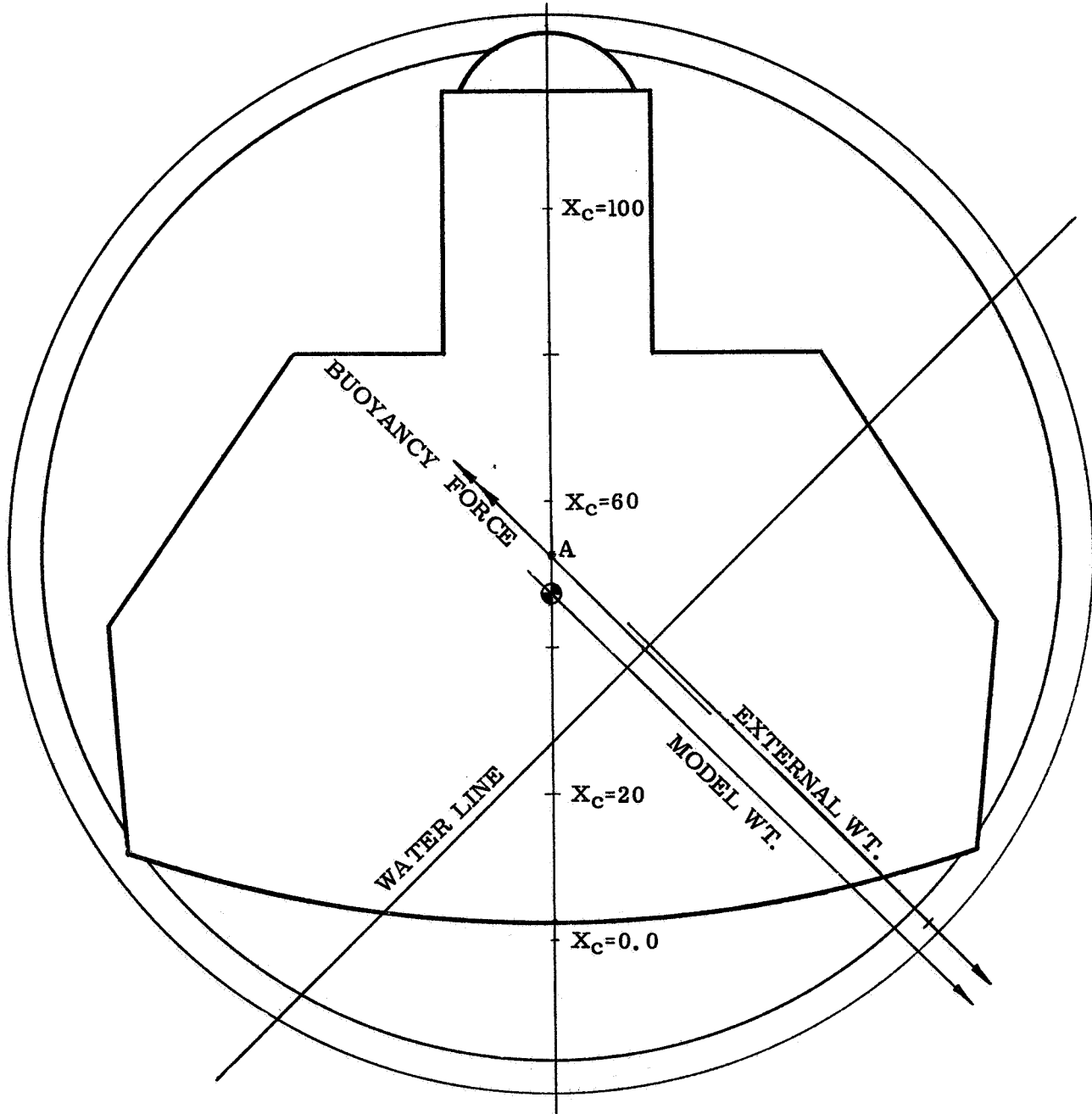


FIG. 5 TYPICAL FORCE DIAGRAM ON PRESSURE VESSEL MODEL DRAWING

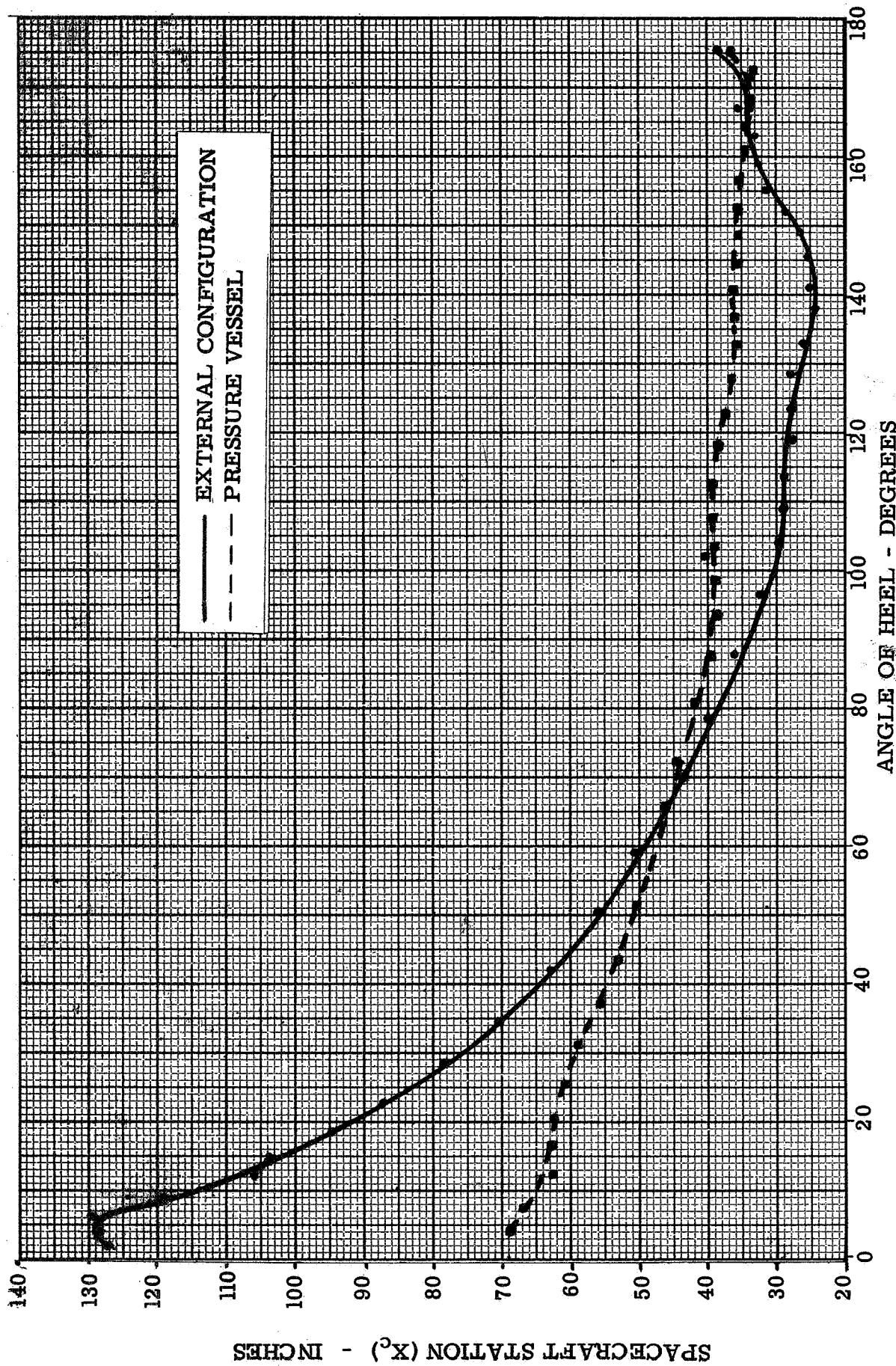


FIG. 6 BUOYANCY FORCE LINES OF ACTION - VERTICAL CENTERLINE INTERSECTION VS ANGLE OF HEEL FOR TEST MODELS AT 8500 POUNDS DISPLACEMENT

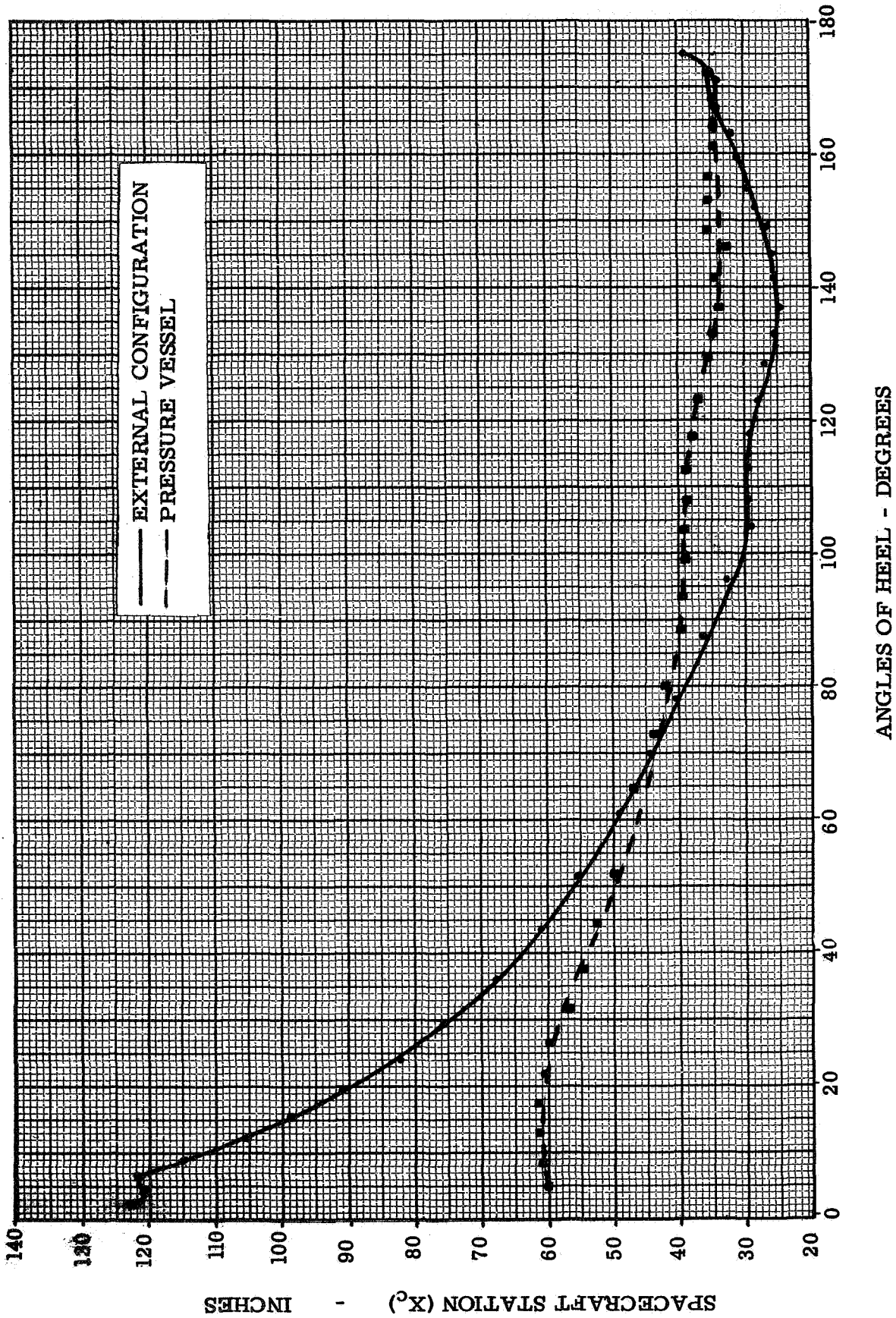
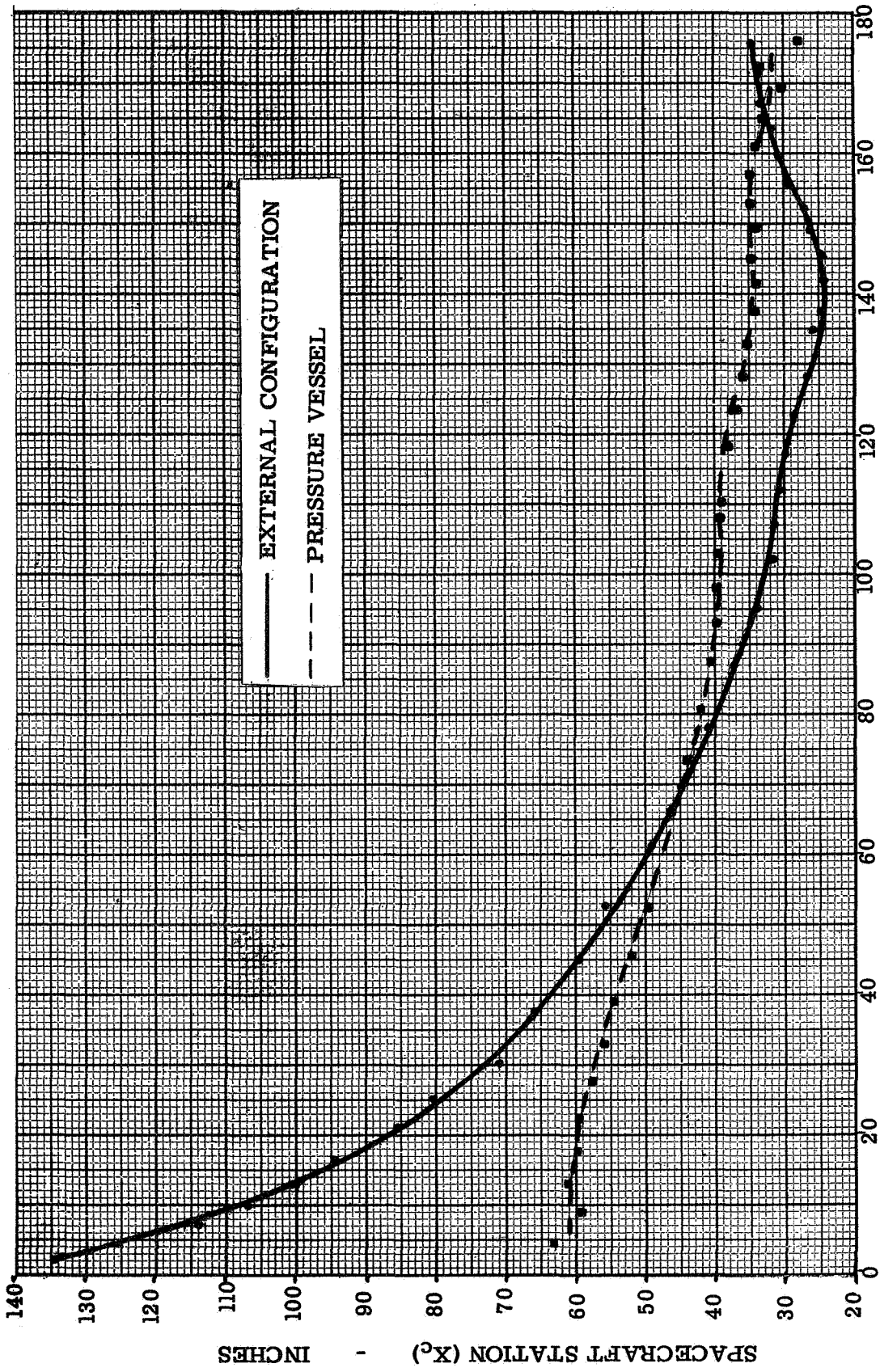


FIG. 7 BUOYANCY FORCE LINES OF ACTION - VERTICAL CENTERLINE INTERSECTION VS ANGLE OF HEEL FOR TEST MODELS AT 9000 POUNDS DISPLACEMENT



ANGLES OF HEEL - DEGREES

FIG. 8 BUOYANCY FORCE LINES OF ACTION - VERTICAL CENTERLINE INTERSECTION VS ANGLE OF HEEL FOR TEST MODELS AT 9500 POUNDS DISPLACEMENT

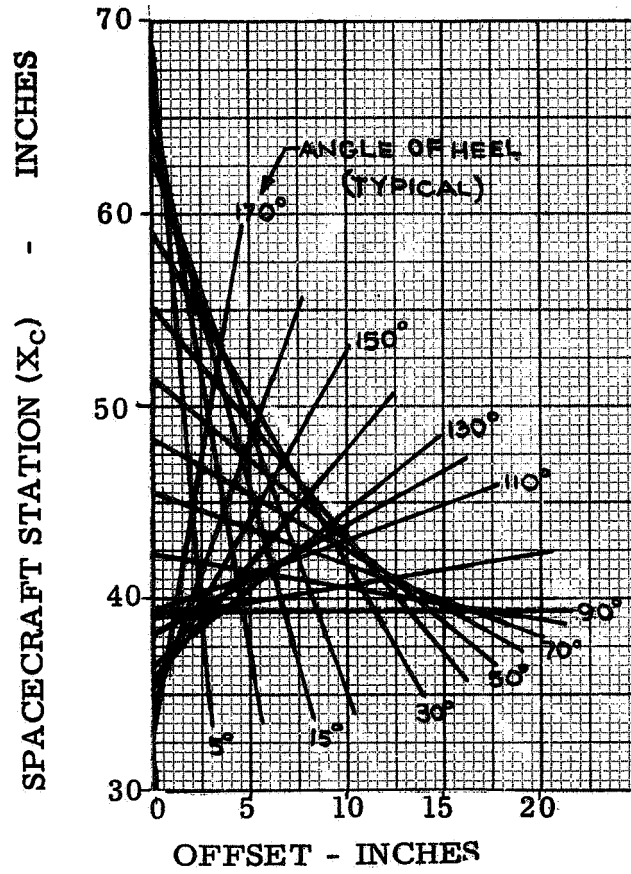


FIG. 9 BUOYANCY FORCE LINES OF ACTION FOR PRESSURE VESSEL AT 8500 POUNDS DISPLACEMENT

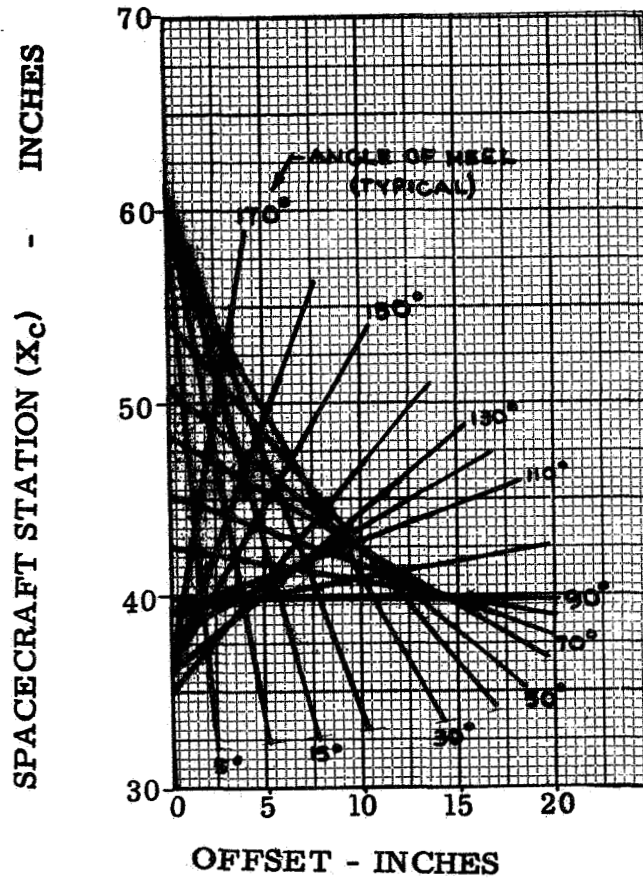


FIG. 10 BUOYANCY FORCE LINES OF ACTION
FOR PRESSURE VESSEL AT 9000 POUNDS
DISPLACEMENT

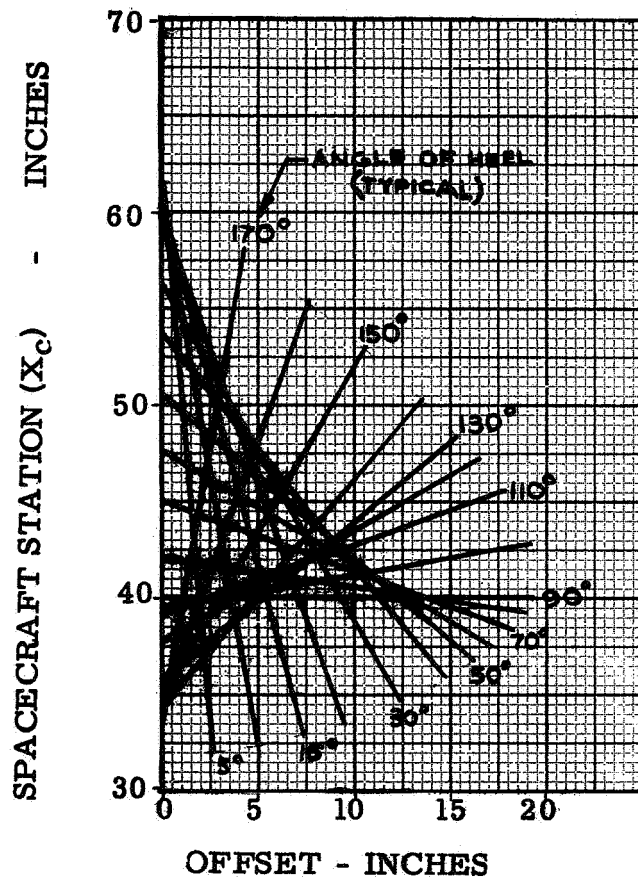


FIG. 11 BUOYANCY FORCE LINES
OF ACTION FOR PRESSURE
VESSEL AT 9500 POUNDS
DISPLACEMENT

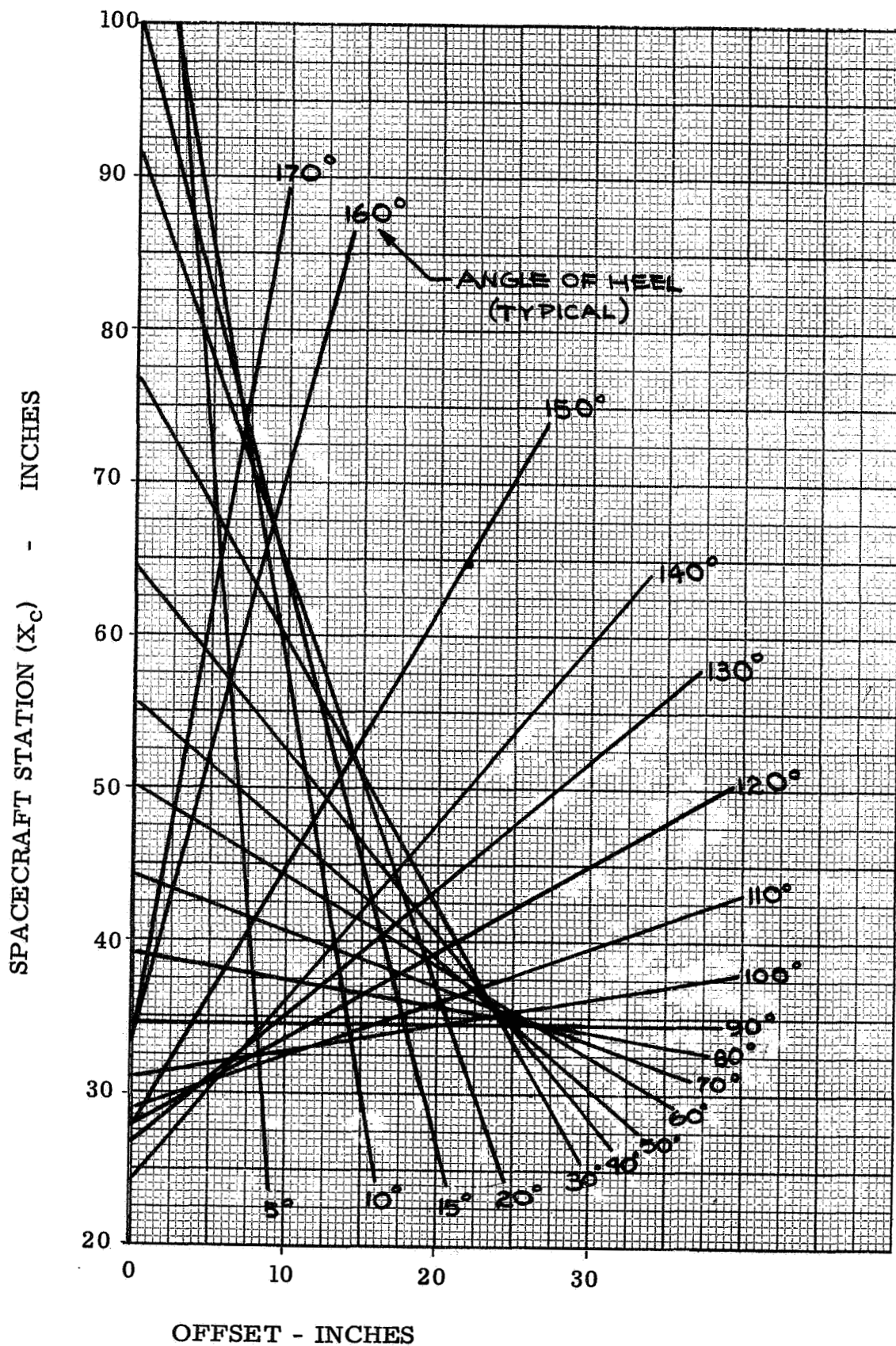


FIG. 12 BUOYANCY FORCE LINES OF ACTION
FOR EXTERNAL CONFIGURATION AT
8500 POUNDS DISPLACEMENT

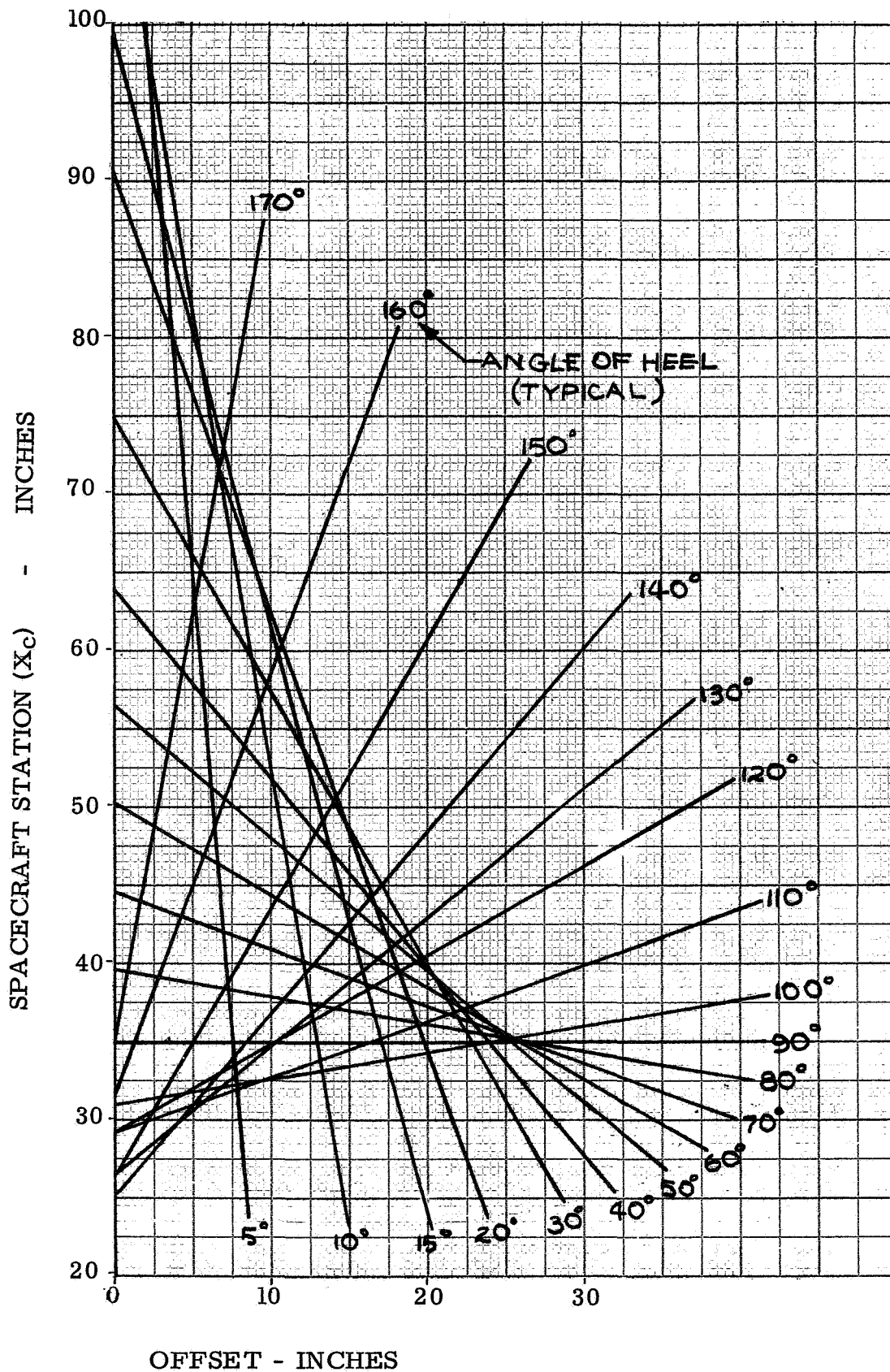


FIG. 13 BUOYANCY FORCE LINES OF ACTION FOR EXTERNAL CONFIGURATION AT 9000 POUNDS DISPLACEMENT

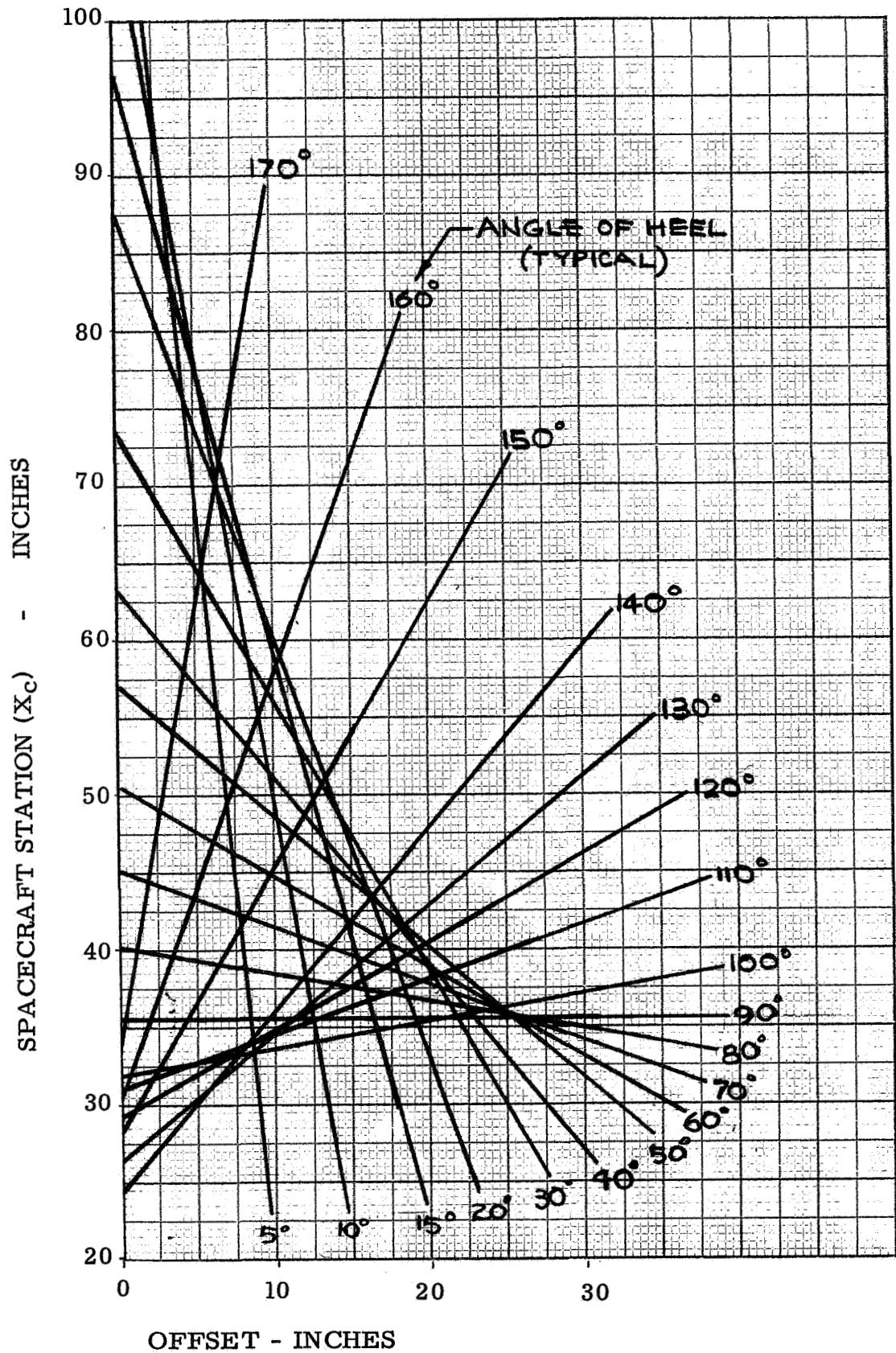


FIG. 14 BUOYANCY FORCE LINES OF ACTION FOR EXTERNAL CONFIGURATION AT 9500 POUNDS DISPLACEMENT

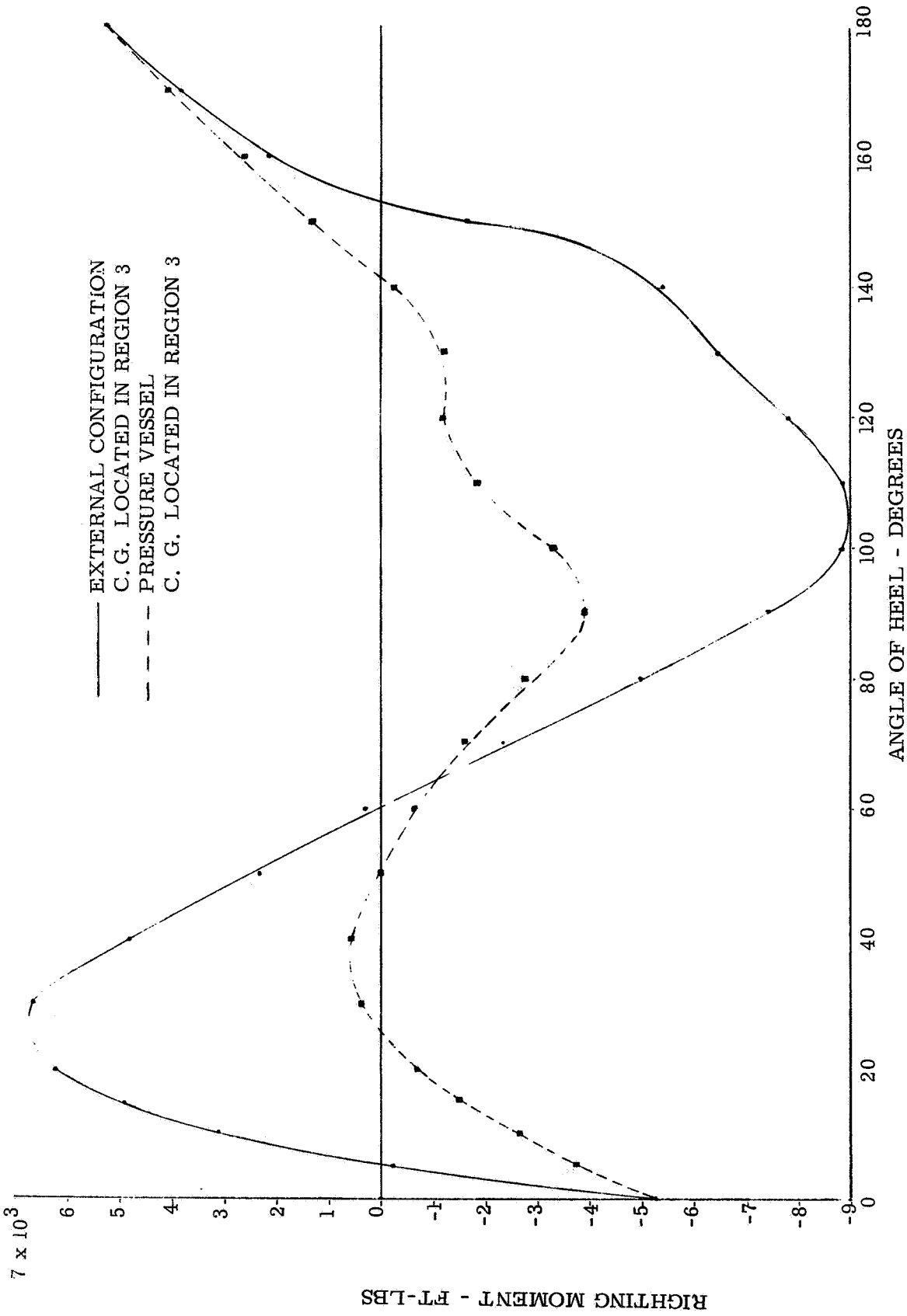


FIG. 15 RIGHTING MOMENT VS ANGLE OF HEEL FOR PRESSURE VESSEL AND EXTERNAL CONFIGURATION AT 8500 POUNDS DISPLACEMENT WITH C. G. LOCATED AT $X_c=45$, OFFSET 7.5 INCHES

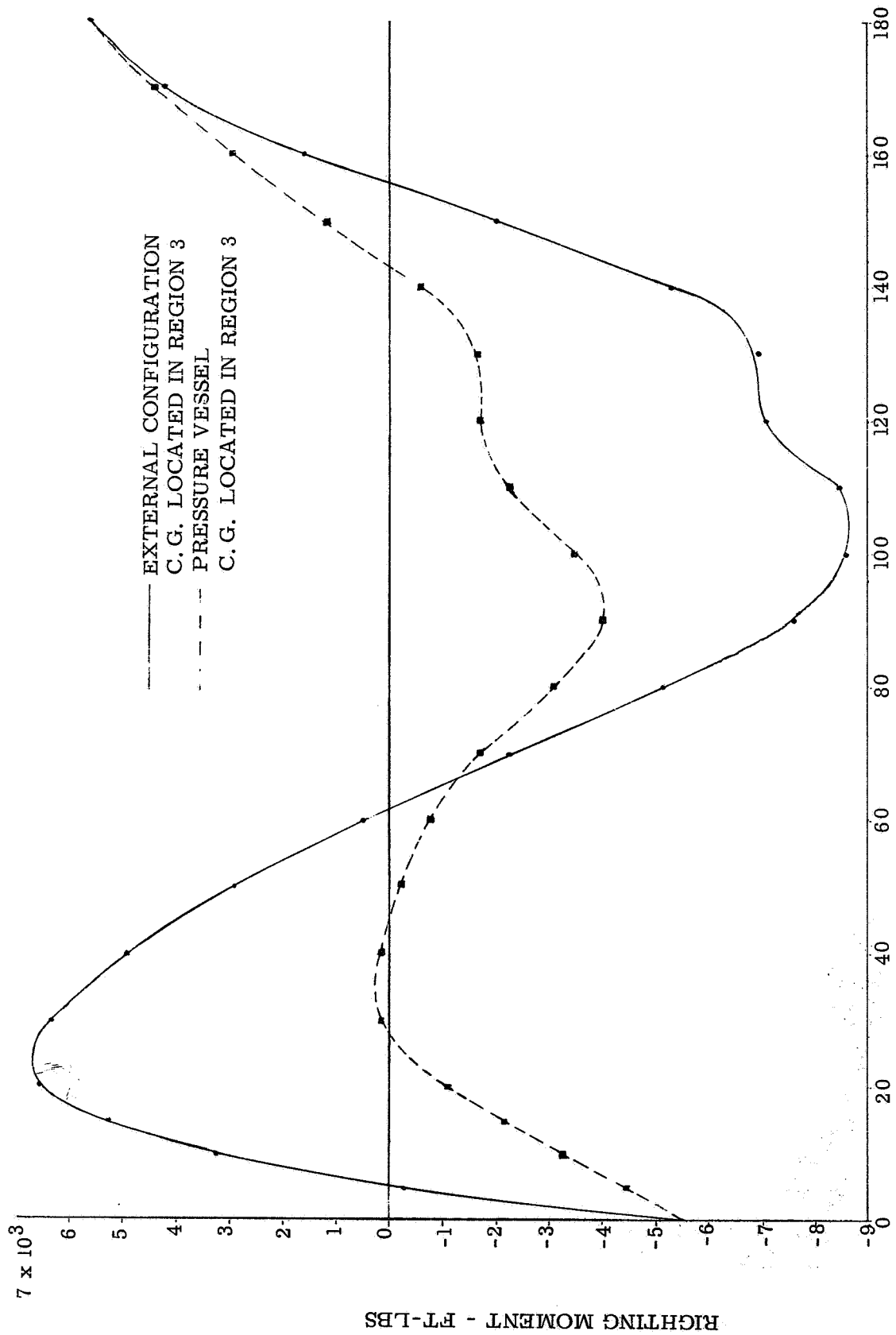


FIG. 16 RIGHTING MOMENT VS ANGLE OF HEEL FOR
 PRESSURE VESSEL, AND EXTERNAL CONFIGURATION
 AT 9000 POUNDS DISPLACEMENT WITH C. G.
 LOCATED AT X_c=45, OFFSET 7.5 INCHES

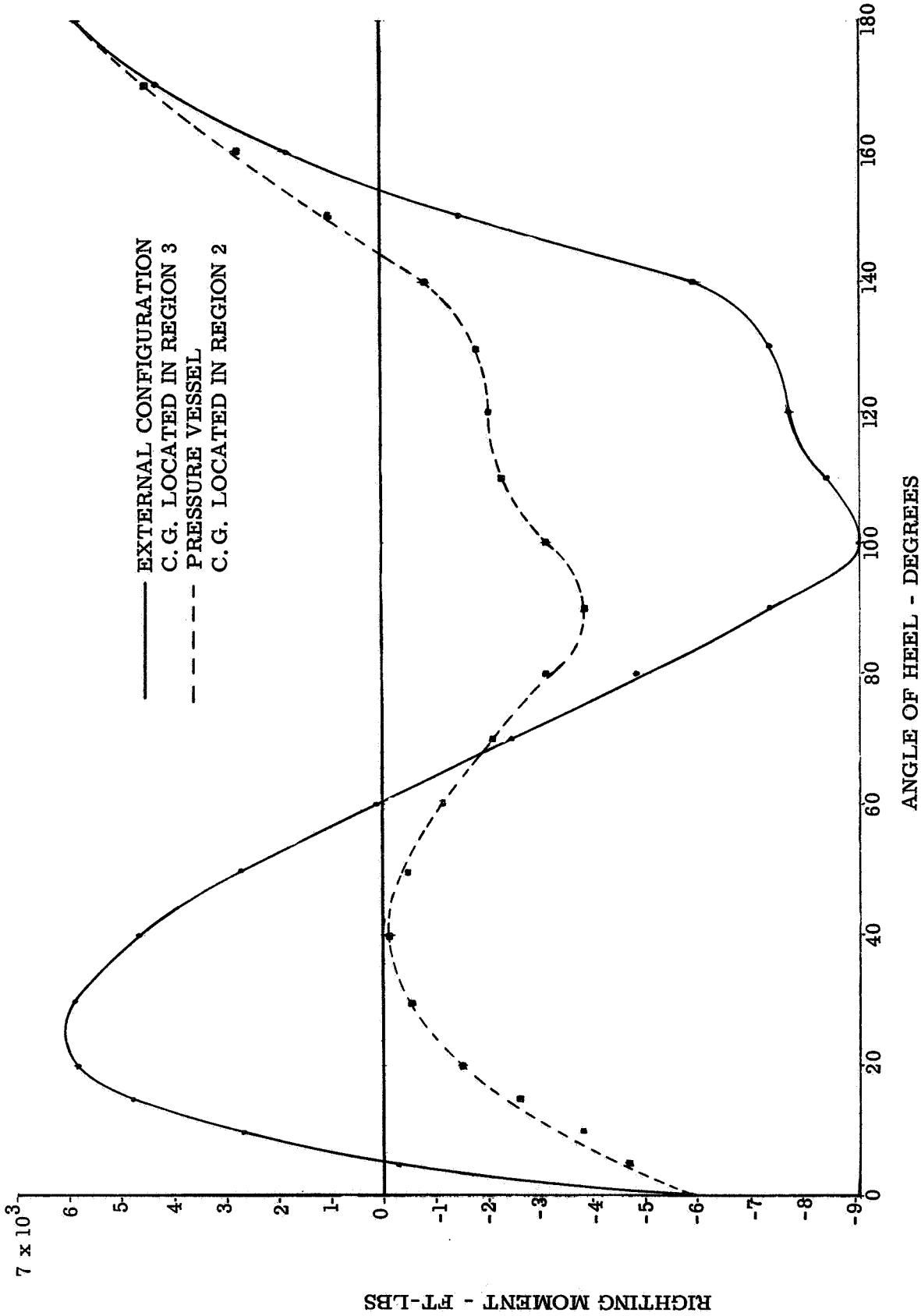


FIG. 17 RIGHTING MOMENT VS ANGLE OF HEEL FOR PRESSURE VESSEL AND EXTERNAL CONFIGURATION AT 9500 POUNDS DISPLACEMENT WITH C. G. LOCATED AT $X_c=45$, OFFSET 7.5 INCHES

- 1 - ONE STABLE ATTITUDE, ANGLE OF HEEL FROM 0° TO 90°
- 2 - ONE STABLE ATTITUDE, ANGLE OF HEEL FROM 90° TO 180°
- 3 - TWO STABLE ATTITUDES, ANGLE OF HEEL FROM 0° TO 90° AND FROM 90° TO 180°

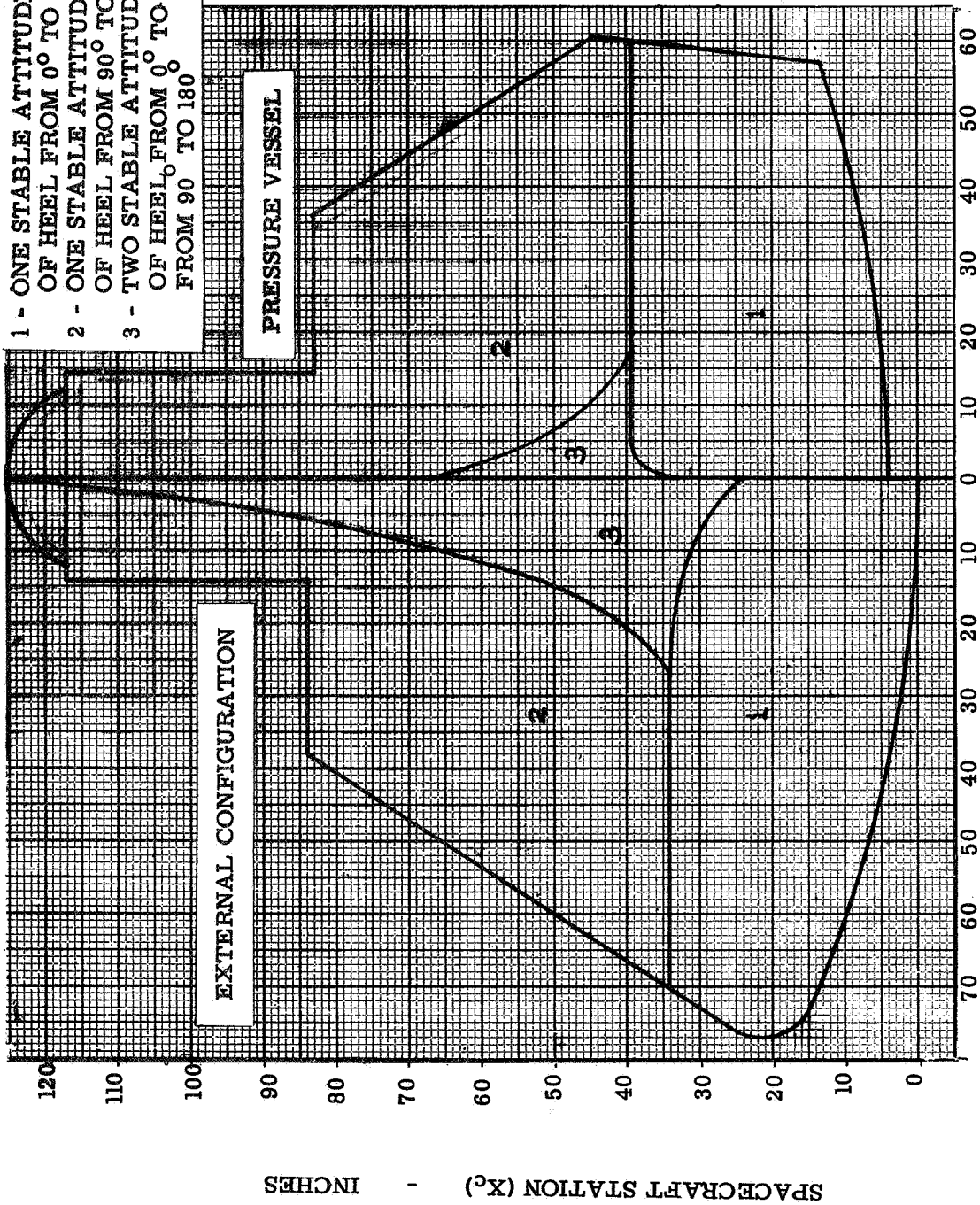


FIG. 18 REGIONS OF SIGNIFICANT C. G. LOCATIONS FOR PRESSURE VESSEL AND EXTERNAL CONFIGURATION AT 8500 POUNDS DISPLACEMENT

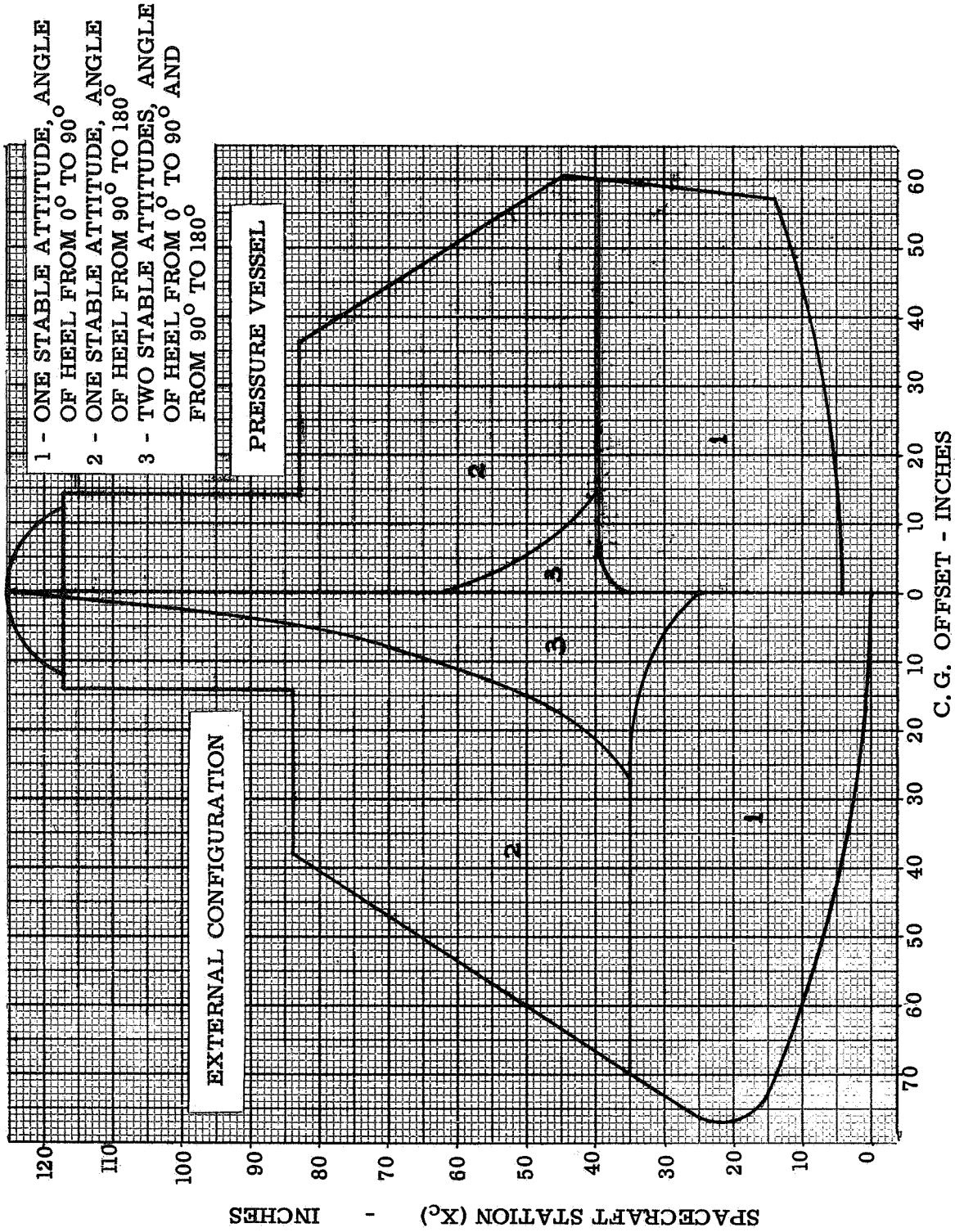


FIG. 19 REGIONS OF SIGNIFICANT C.G. LOCATIONS FOR PRESSURE VESSEL AND EXTERNAL CONFIGURATION AT 9000 POUNDS DISPLACEMENT

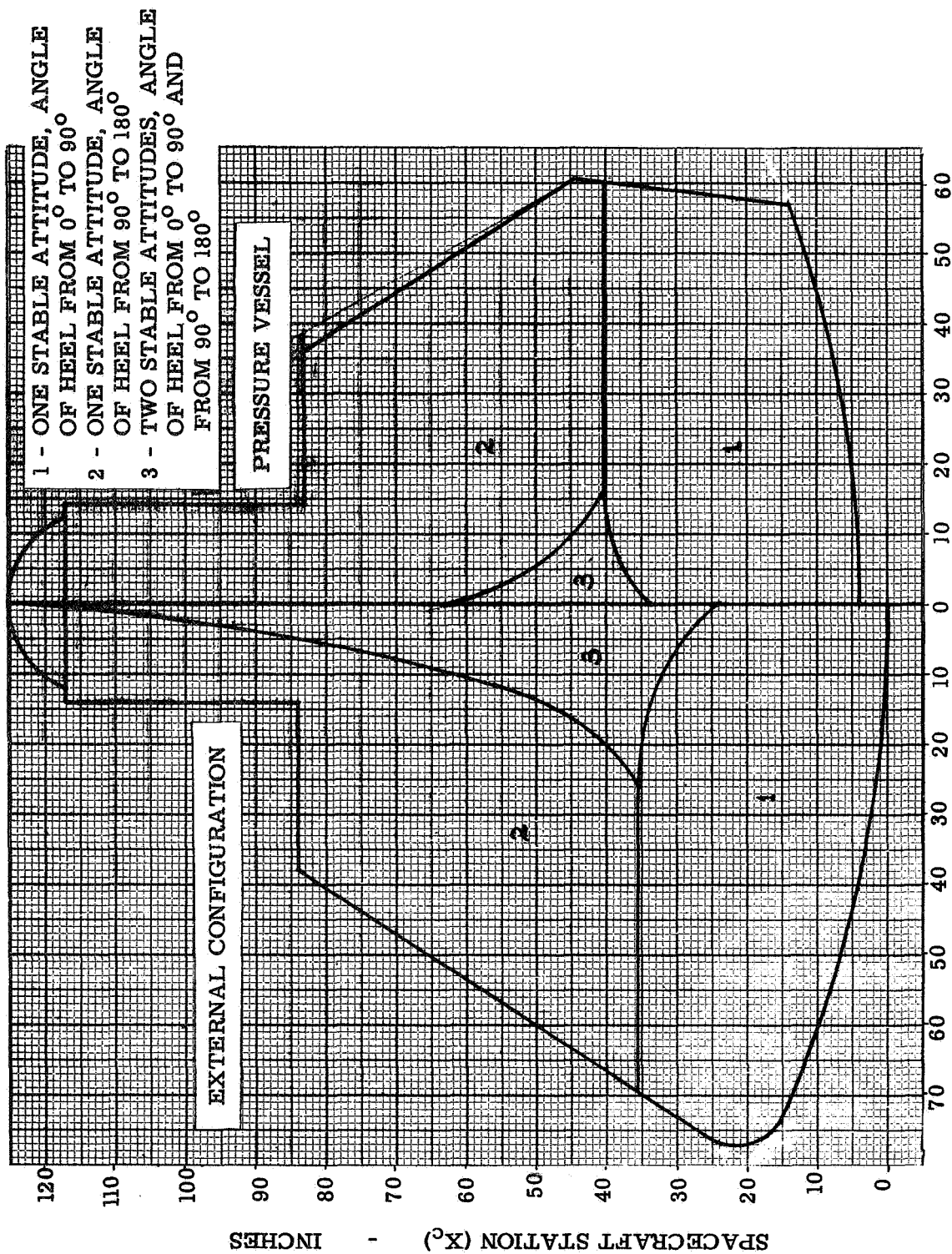


FIG. 20 REGIONS OF SIGNIFICANT C.G. LOCATIONS FOR PRESSURE VESSEL AND EXTERNAL CONFIGURATION AT 9500 POUNDS DISPLACEMENT

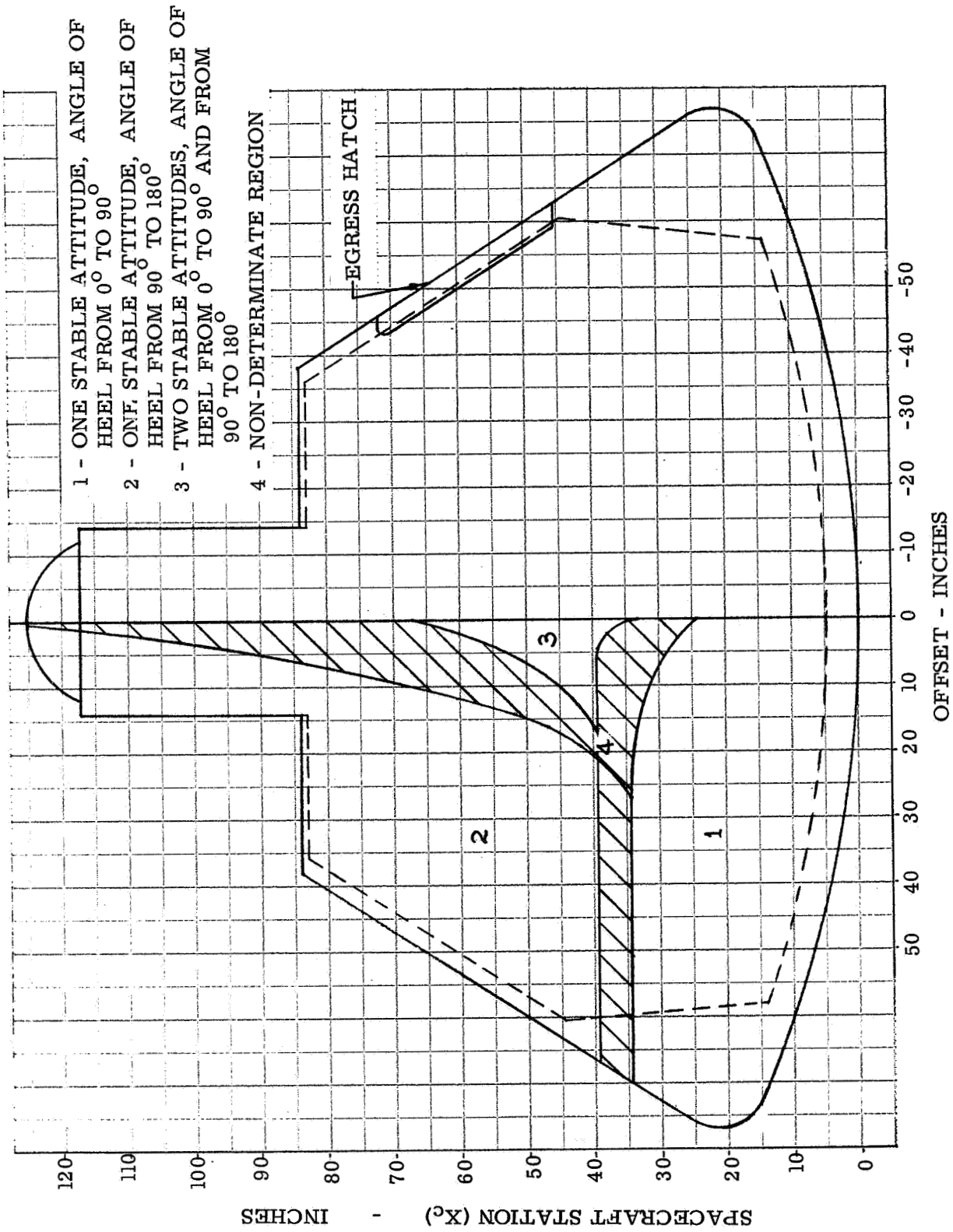


FIG. 21 C.G. REGIONS OF DETERMINATE AND NON-DETERMINATE ATTITUDES AT 8500 POUNDS DISPLACEMENT

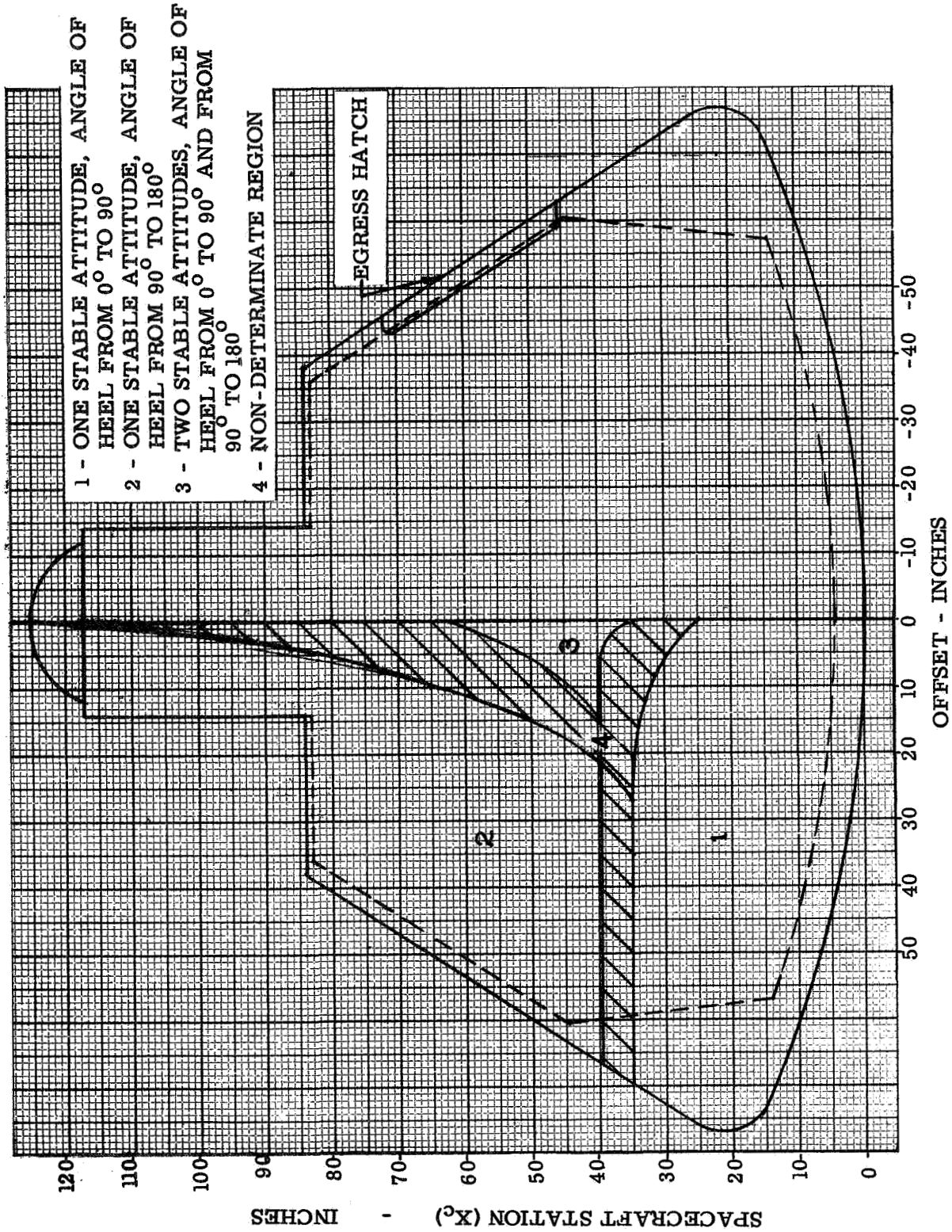


FIG. 22 C.G. REGIONS OF DETERMINATE AND NON-DETERMINATE ATTITUDES AT 9000 POUNDS DISPLACEMENT

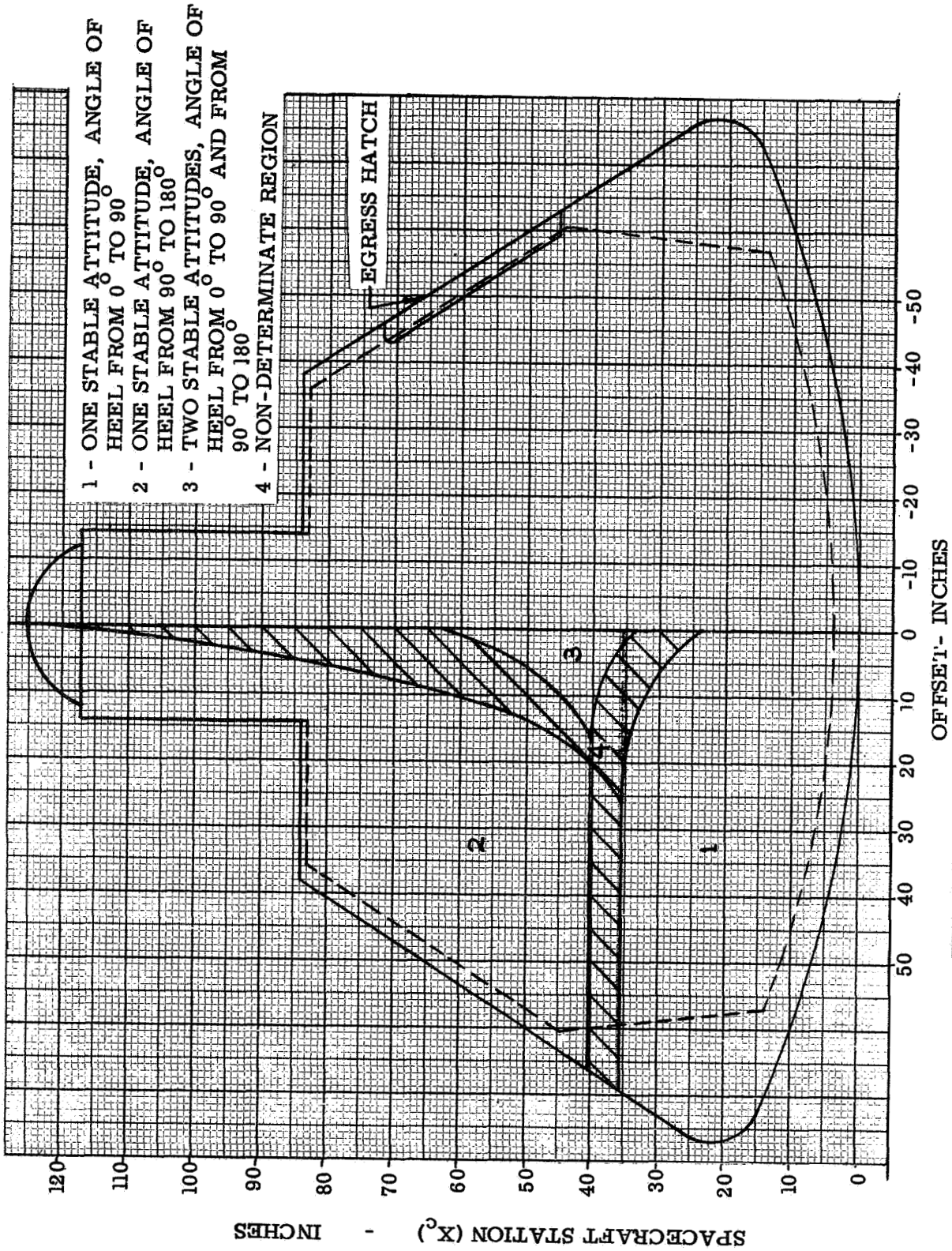
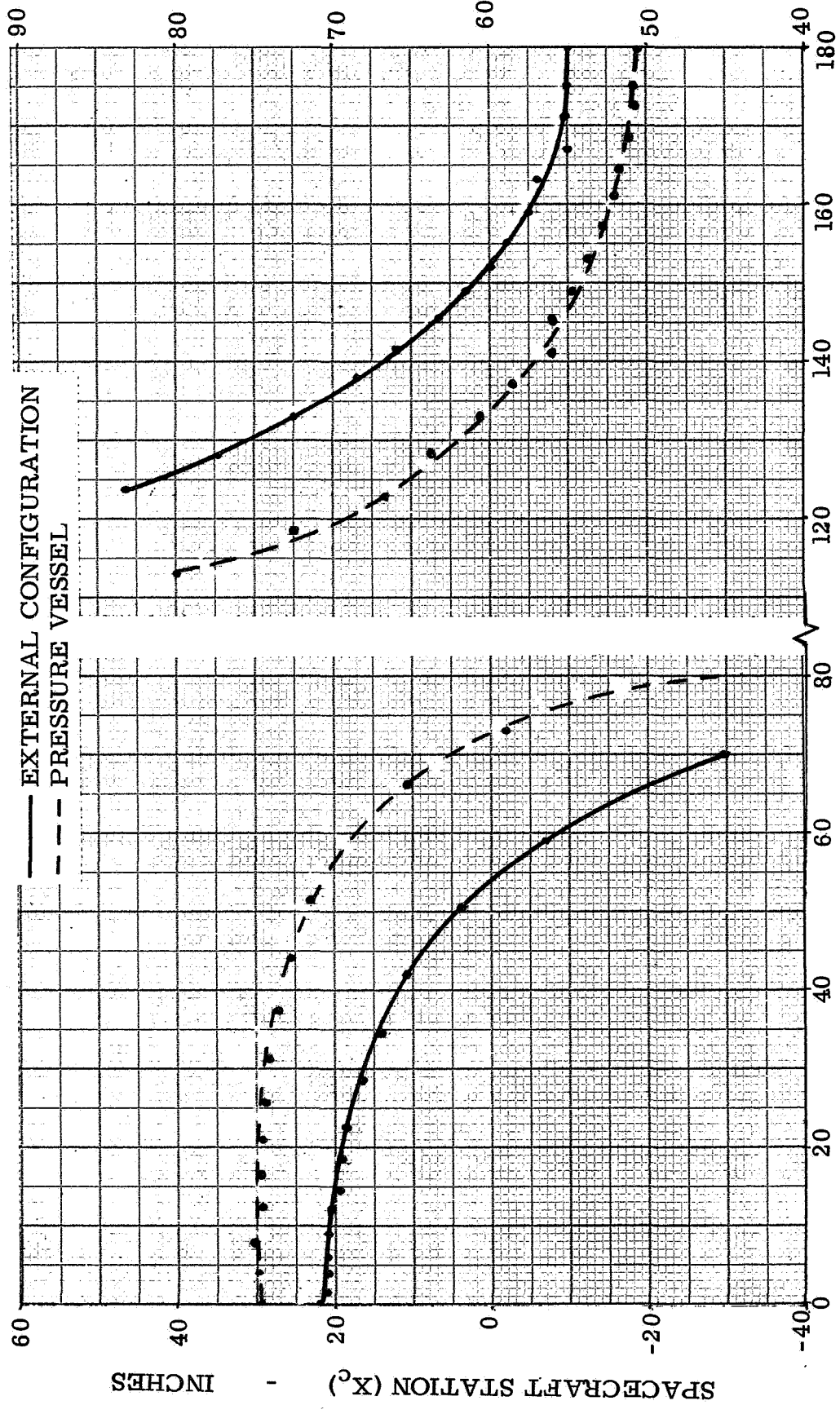


FIG. 23 C.G. REGIONS OF DETERMINATE AND NON-DETERMINATE ATTITUDES AT 9500 POUNDS DISPLACEMENT



ANGLE OF HEEL - DEGREES

FIG. 24 WATERLINE AND SPACECRAFT CENTERLINE INTERSECTION AT 8500 POUNDS DISPLACEMENT

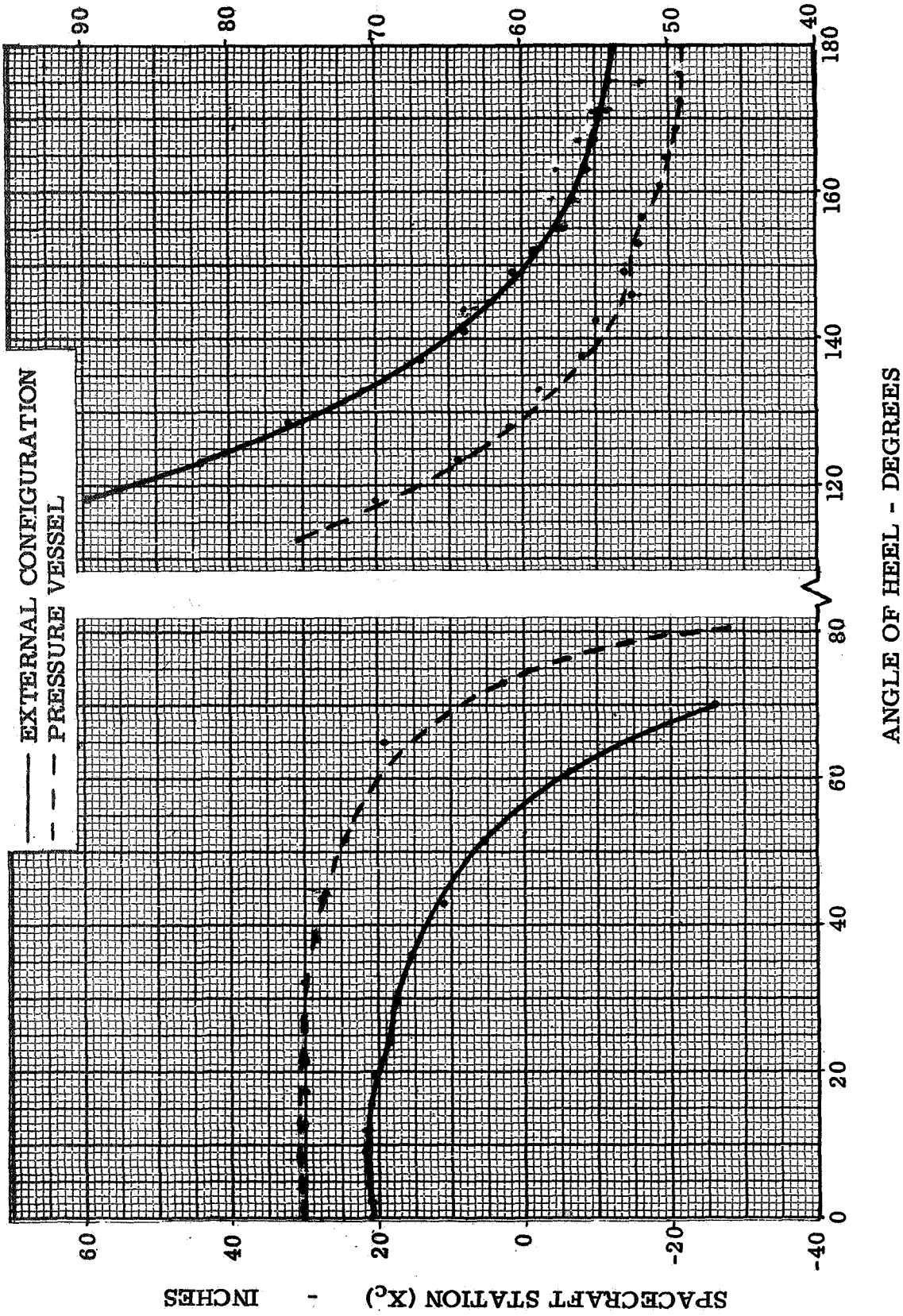


FIG. 25 WATERLINE AND SPACECRAFT CENTERLINE INTERSECTION AT 9000 POUNDS DISPLACEMENT

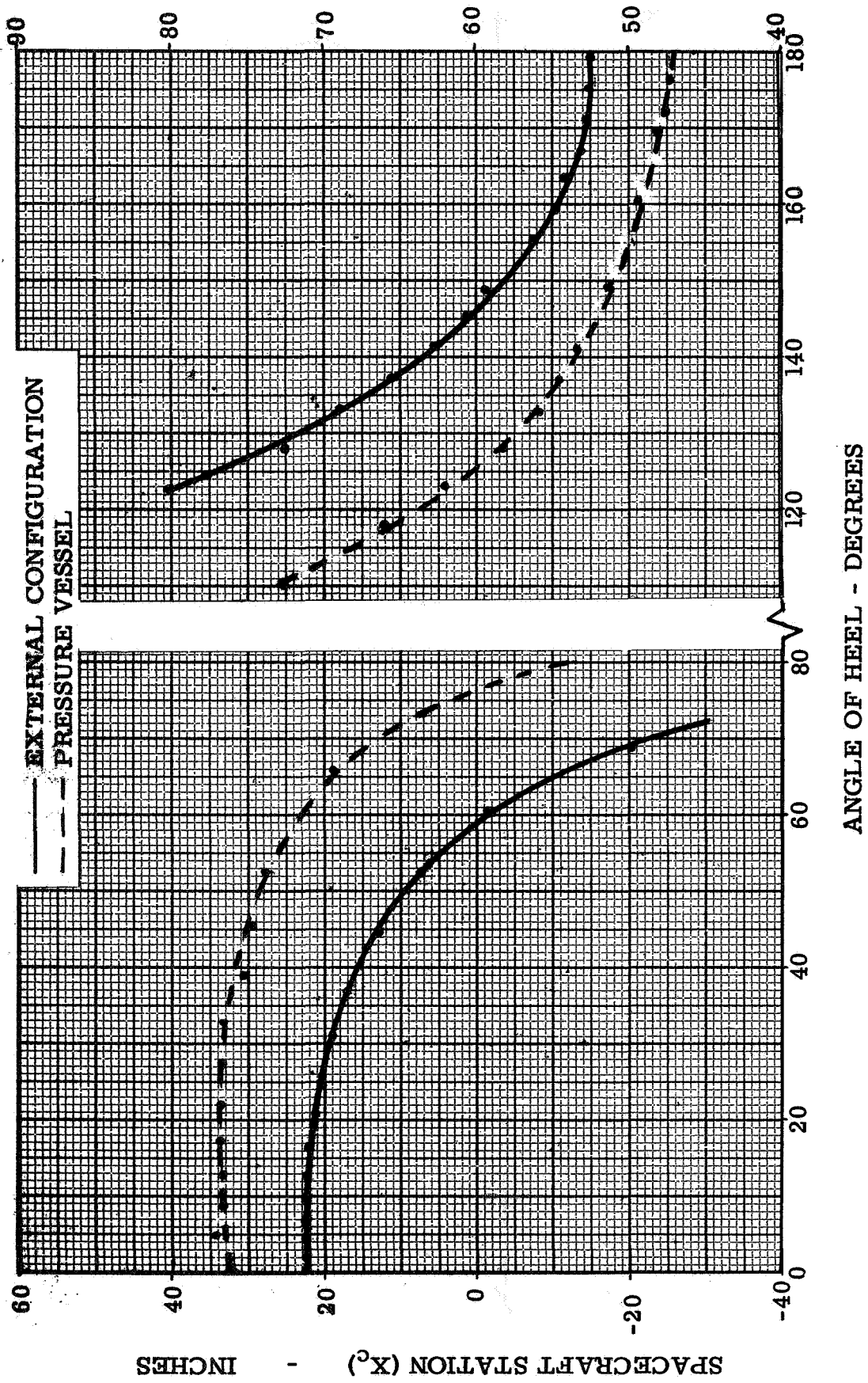


FIG. 26 WATERLINE AND SPACECRAFT CENTERLINE INTERSECTION AT 9500 POUNDS DISPLACEMENT

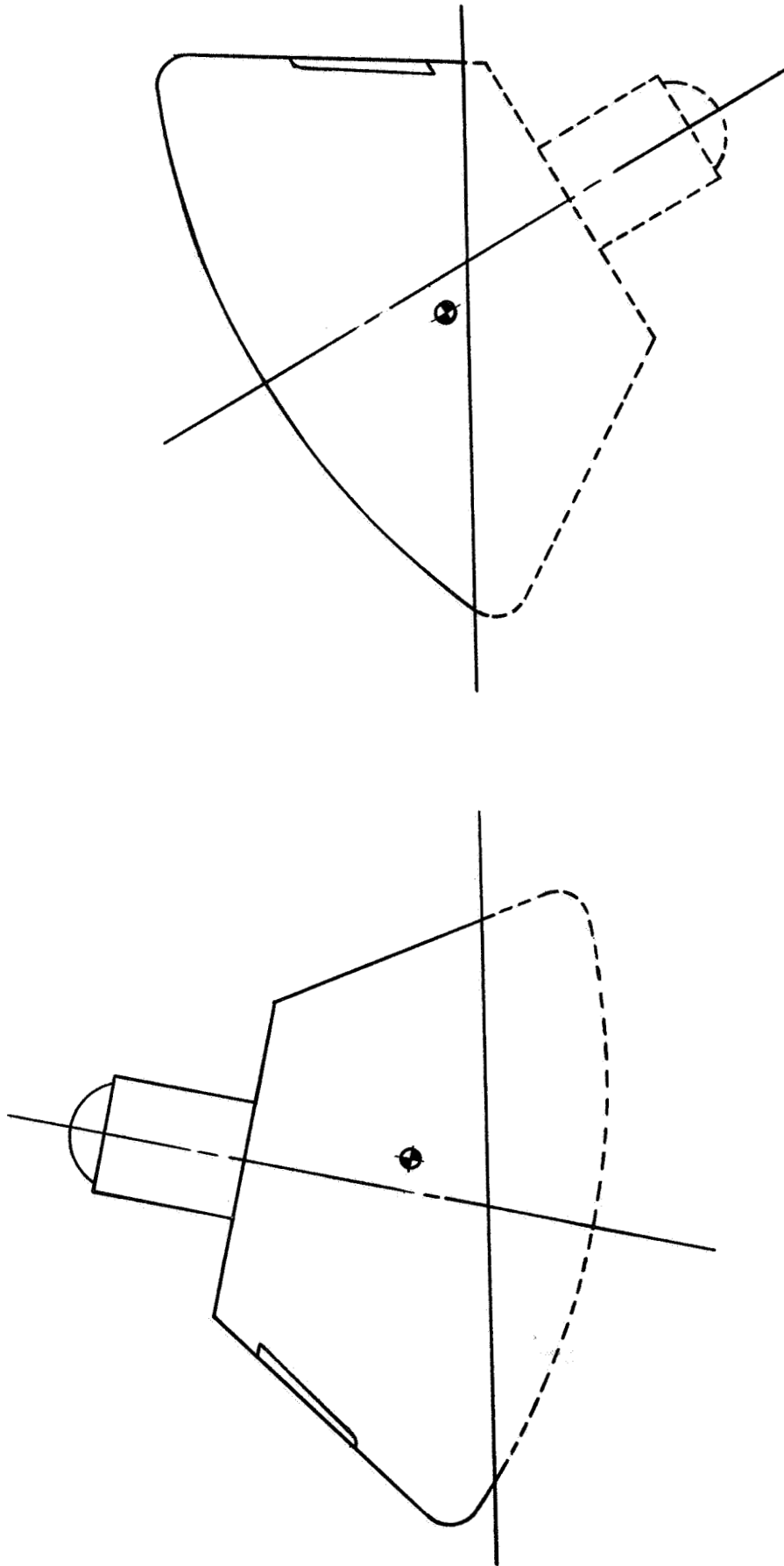


FIG. 27 TYPICAL APOLLO FLOTATION ATTITUDES AND HATCH EXPOSURE AT 9000 POUNDS DISPLACEMENT WITH C.G. LOCATED AT $X_c=45$, OFFSET 7.5 INCHES

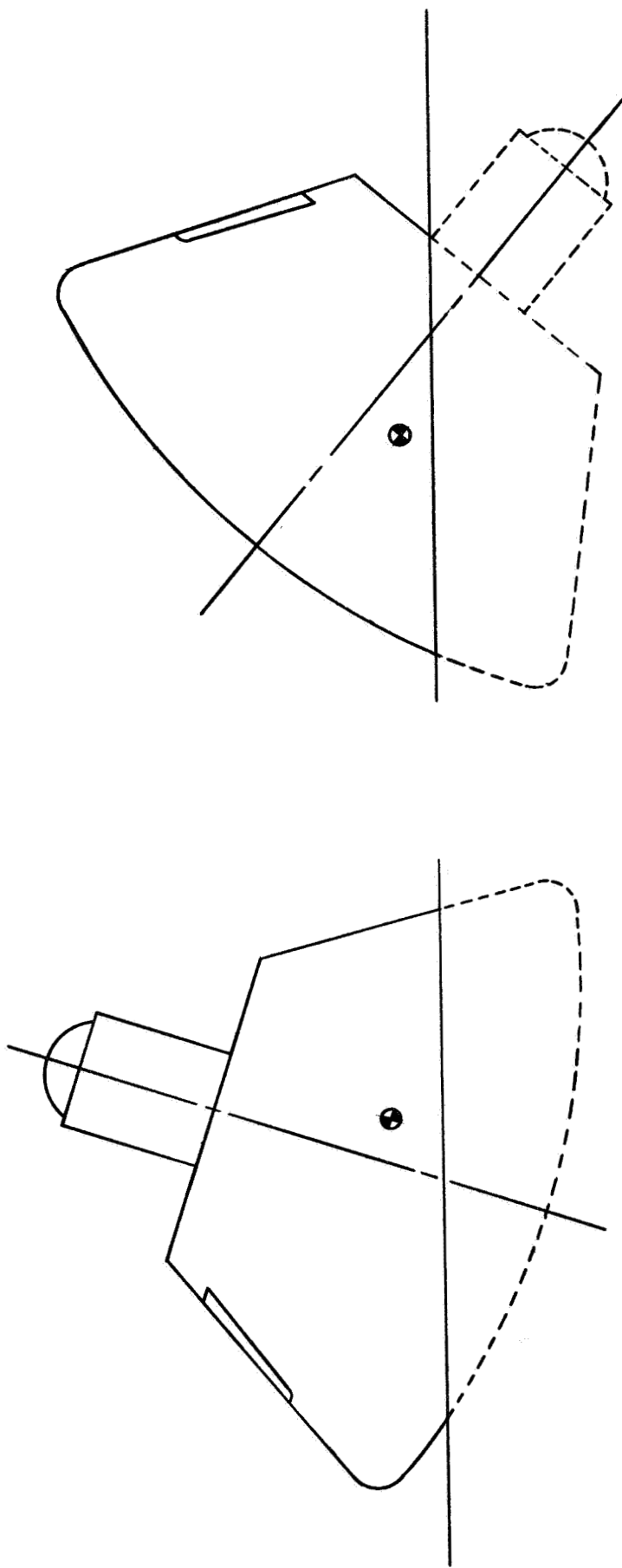


FIG. 28 TYPICAL APOLLO FLOTATION ATTITUDES
AND HATCH EXPOSURE AT 9000 POUNDS
DISPLACEMENT WITH C. G. LOCATED
AT $X_c = 42$, OFFSET 10 INCHES